

Dual-Mode Adaptive Neural Observer Design for Pure-Feedback Switched Nonlinear Systems with Hybrid Measurement Defects

Zhongfeng Li, Lidong Wang, Lu Liang, Lei Liu*, and Zhenlong Zhao*

Abstract—This paper addresses the control challenge for switched nonlinear pure-feedback systems (SNPS) under measurement imperfections and uncertain dynamics. A neural observer framework simultaneously handles state estimation and unknown function approximation during measurement defects, including data loss and sensor saturation. Utilizing the mean value theorem, the non-affine structure is transformed to enable systematic backstepping synthesis without linearization. Dual adaptive strategies for normal operation and data-loss scenarios are unified via probabilistic measurement modeling. Stability guarantees are established through average dwell-time constraints and switched Lyapunov analysis, proving uniform ultimate boundedness (UUB) of all closed-loop signals. Benchmark simulations demonstrate the controller's efficacy in maintaining tracking performance amid intermittent measurements and subsystem switching. This approach extends existing methods by integrating neural approximation, switching logic, and defect compensation into a unified architecture.

Index Terms—Switched nonlinear pure-feedback system, incomplete measurements, average dwell-time, uniformly ultimately bounded.

I. INTRODUCTION

SWITCHED nonlinear systems, characterized by interactions between continuous dynamics and discrete switching events [1], have become a focal point in modern control theory [2]. Originating from hybrid system concepts pioneered by Nerode and Antsaklis, such

systems find applications ranging from power electronics to autonomous vehicles [3]. The inherent complexity of these systems arises from their multiple subsystems governed by switching signals, necessitating specialized control strategies [4–6]. Recent advancements in adaptive backstepping techniques and common Lyapunov function approaches have significantly enhanced state-feedback controller designs [7, 8], particularly for systems with unstable dynamics [9].

Pure-feedback architectures present unique challenges compared to their strict-feedback counterparts due to the absence of affine state variables in control inputs [10]. This structural characteristic complicates both virtual and actual controller design, especially when handling output constraints and stochastic disturbances [11, 12]. Contemporary studies have addressed these challenges through nonlinear mapping techniques and adaptive tracking control under arbitrary switching [13], yet critical gaps remain in handling incomplete measurements and uncertain dynamics.

Real-world implementations frequently encounter measurement imperfections caused by network-induced data loss and sensor saturation [14]. While shared communication networks reduce wiring complexity, packet loss and transmission delays degrade system performance [15]. Existing solutions predominantly address either normal operating conditions or isolated data loss scenarios [16], lacking comprehensive frameworks that simultaneously handle measurement saturation, data dropout, and subsystem switching. This limitation becomes particularly apparent in safety-critical applications requiring robust performance under multiple concurrent disturbances.

This study advances the field through four principal innovations:

- **Composite measurement modeling:** Unlike conventional approaches that treat data loss and saturation separately [17], we introduce coupled stochastic variables to unify these phenomena, enabling simultaneous handling of perfect and defective measurements through probabilistic analysis.
- **Non-affine transformation:** Leveraging the mean value theorem, we resolve the intrinsic non-affine property of pure-feedback systems, permitting systematic backstepping controller synthesis without restrictive linearization assumptions.
- **Switching logic integration:** By incorporating average dwell-time constraints [16] with probabilistic stability criteria, we establish sufficient conditions for uniform ultimate boundedness under arbitrary switching signals

Manuscript received May 1, 2025; revised July 18, 2025.

This work was supported in part by the Fundamental Research Funds for Liaoning Provincial Joint Funds Project - General Funding Program (Grant Nos. 2023-MSLH-323 and 2023-MSLH-310); the Fundamental Research Funds for Liaoning Universities (Grant No. LJ212410146009); 2025 scientific research fund project of Liaoning Provincial Department of Education (Grant No. LJ212514435004 and Grant No. LJ212514435006); 2022 scientific research fund project of Liaoning Provincial Department of Education (Grant No. LJKFZ20220292 and Grant No. LJKMZ20221859); the Foundation of Yingkou Automation Industrial Control Professional Technology Innovation Center (Grant No. AICPTI02); the Foundation of Yingkou Institute of Technology under the Institutional-Level Scientific Research Initiative (Grant Nos. FDL202404 and FDL202409).

Zhongfeng Li is an associate professor at the School of Electrical Engineering, Yingkou Institute of Technology, Yingkou 115100 China (e-mail: afeng0601@163.com).

Lidong Wang is a professor at the School of Electronic and Information Engineering, University of Science and Technology Liaoning, Anshan 114051 China (e-mail: wangld5600@163.com).

Lu Liang is a postgraduate of School of Electronic and Information Engineering, University of Science and Technology Liaoning, Anshan 114051 China (e-mail: 981330217@qq.com).

Lei Liu is an associate professor at the School of Mechanical Engineering, Yingkou Institute of Technology, Yingkou 115100 China (corresponding author, e-mail: liulei@yku.edu.cn).

Zhenlong Zhao is an associate professor at the School of Electrical Engineering, Yingkou Institute of Technology, Yingkou 115100 China (corresponding author, e-mail: zhaozhenlong@yku.edu.cn).

and intermittent measurements.

- **Hybrid estimation strategy:** A switched neural observer architecture is developed, combining radial basis function networks for unknown dynamics approximation with adaptive laws that differ between normal and data-loss operation modes, overcoming the complete state measurement assumption prevalent in existing works.

The subsequent sections are organized as follows: Section II formulates the switched pure-feedback system with measurement imperfections and introduces neural network preliminaries. Section III details the observer-based backstepping controller design for both measurement scenarios. Stability analysis via multiple Lyapunov functions and dwell-time constraints appears in Section IV, followed by comparative simulation studies in Section V. Concluding remarks and future directions complete the paper.

Notations: \mathbb{R}^n denotes n -dimensional Euclidean space. The operator $\|\cdot\|$ represents the Euclidean norm for vectors and the induced 2-norm for matrices. $\lambda_{\{\min, \max\}}(\cdot)$ extracts extreme eigenvalues of symmetric matrices. $\mathbb{E}[\cdot]$ and $\mathbb{D}[\cdot]$ denote expectation and variance operators, respectively. The Hermitian operator $\text{He}(P) = P + P^\top$ applies to square matrices. Time derivatives appear as $y_d^{(k)} = d^k y_d / dt^k$ for the reference signal $y_d(t)$. The diagonal matrix I_k contains unity at the k -th position and zeros elsewhere [18].

II. SYSTEM MODELING AND PRELIMINARIES

Consider a class of uncertain switched nonlinear systems in pure-feedback form with partial state information, governed by:

$$\begin{aligned} \dot{x}_1 &= f_{1\sigma}(x_1, x_2) + d_{1\sigma}(t) \\ &\vdots \\ \dot{x}_{n-1} &= f_{n-1,\sigma}(\bar{x}_{n-1}, x_n) + d_{n-1,\sigma}(t) \\ \dot{x}_n &= f_{n\sigma}(\bar{x}_n, u_\sigma) + d_{n\sigma}(t) \\ y &= \sum_{k=1}^3 \rho_k \psi_k(x_1), \end{aligned} \quad (1)$$

where $x_i \in \mathbb{R}$ represents the system states, $u_\sigma \in \mathbb{R}$ is the subsystem-specific control input, and $\sigma(t) : \mathbb{R}^+ \rightarrow \mathcal{M} = \{1, \dots, m\}$ is the switching signal. The measurement conditions are given by $\rho_1 + \rho_2 + \rho_3 = 1$, with $\rho_k \in \{0, 1\}$, where $\psi_1(x_1) = x_1$, $\psi_2(x_1) = \text{sat}(x_1)$, and $\psi_3(x_1) = x'_1$ represent normal measurement, saturation, and data-loss compensation, respectively. The unknown disturbances $d_{i\sigma}(t)$ satisfy $|d_{i\sigma}(t)| \leq \bar{d}_{i\sigma}$.

The non-affine structure of the system complicates controller synthesis. To address this, we apply the mean value theorem [19]:

$$f_{i\sigma}(\bar{x}_i, x_{i+1}) = f_{i\sigma}(\bar{x}_i, 0) + h_{\mu i} x_{i+1}, \quad (2)$$

where $h_{\mu i} = \frac{\partial f_{i\sigma}}{\partial x_{i+1}}|_{x_{i+1}=x_{\mu i}}$ with $x_{\mu i} \in (0, x_{i+1})$. This yields the transformed dynamics:

$$\begin{aligned} \dot{x}_1 &= f_{1\sigma}(x_1) + h_{\mu 1} x_2 + d_{1\sigma} \\ &\vdots \\ \dot{x}_n &= f_{n\sigma}(\bar{x}_n) + h_{\mu n} u_\sigma + d_{n\sigma} \\ y &= \sum_{k=1}^3 \rho_k \psi_k(x_1). \end{aligned} \quad (3)$$

Measurement modes operate as:

- Normal mode ($\rho_1 = 1$): $y = x_1$
- Saturation mode ($\rho_2 = 1$): $y = \text{sign}(x_1) \min(|x_1|, x_{\max})$
- Data-loss mode ($\rho_3 = 1$): $y = x'_1$ (last valid sample)

The switching logic follows average dwell-time (ADT) constraints [20]:

$$N_\sigma(T) \leq N_0 + \frac{T}{\tau_a}, \quad \forall T > 0, \quad (4)$$

where $N_\sigma(T)$ counts switchings in $[0, T)$, and τ_a denotes the minimum ADT. Control objectives require:

$$\limsup_{t \rightarrow \infty} |y(t) - y_d(t)| \leq \Upsilon, \quad (5)$$

with $y_d(t)$ being the reference trajectory. Key assumptions include:

Assumption 2.1: The reference signal $y_d(t)$ and its n derivatives remain bounded with $\|y_d^{(k)}\| \leq Y_k$, $k = 0, \dots, n$.

Assumption 2.2: Parameters $h_{\mu i}$ remain positive and bounded: $0 < \underline{h}_i \leq h_{\mu i} \leq \bar{h}_i < \infty$.

Assumption 2.3: The unknown functions $f_{i\sigma}$ satisfy the Lipschitz condition:

$$\|f_{i\sigma}(X) - f_{i\sigma}(X')\| \leq q_i \|X - X'\|, \quad \forall X, X' \in \mathbb{R}^i. \quad (6)$$

Radial basis function networks (RBFNs) approximate unknown nonlinearities:

$$f(Z) = W^T S(Z) + \delta(Z), \quad \|\delta(Z)\| \leq \epsilon, \quad (7)$$

where $S(Z) = [s_1(Z), \dots, s_l(Z)]^T$ uses Gaussian basis functions:

$$s_j(Z) = \exp\left(-\frac{\|Z - \kappa_j\|^2}{2\phi_j^2}\right),$$

centered at $\kappa_j \in \mathbb{R}^n$ with width $\phi_j > 0$. The universal approximation property [21] ensures arbitrary accuracy with a sufficient number of nodes l .

III. CONTROLLER DESIGN AND STABILITY ANALYSIS

In systems exhibiting saturation or data loss, we address how measurements behave when the system experiences saturation, where the previous measurement is retained, or when data loss occurs, where missing data is replaced with the most recent valid observation. These two cases can be unified under the concept of "data loss," where the last valid measurement is used to replace the current value. Thus, we consider the design of state estimators and controllers under two scenarios: normal operation and data loss.

A. Estimator and Backstepping Control Under Normal Measurement Mode

In the normal case, where the state variables of system (3) are not directly measurable, we introduce a state estimator. The estimator is defined as:

$$\begin{aligned}\dot{\hat{x}}_{c1} &= f_{1\sigma(t)}(\hat{x}_{c1}) + h_{\mu1}\hat{x}_{c2} + l_{1\sigma(t)}(y - \hat{x}_{c1}) \\ &\vdots \\ \dot{\hat{x}}_{ci} &= f_{i\sigma(t)}(\hat{x}_{ci}) + h_{\mu i}\hat{x}_{c,i+1} + l_{i\sigma(t)}(y - \hat{x}_{c1}) \\ \dot{\hat{x}}_{cn} &= f_{n\sigma(t)}(\hat{x}_{cn}) + h_{\mu n}u + l_{n\sigma(t)}(y - \hat{x}_{c1}),\end{aligned}\quad (8)$$

where $\hat{x}_{ci}, i = 1, \dots, n$ are the state estimates in the normal case, and $y = x_1$ represents the system output. The control input for the k -th subsystem is u_k , where $k \in M$. The switching signal $\sigma(t)$ is defined as previously, with design parameters $l_{i,k}, i = 1, \dots, n, k \in M$.

Let $e_c = \bar{x}_n - \hat{x}_{cn}$ denote the estimation error in the normal case, with the first component $e_{11} = y - \hat{x}_{c1}$. Using equations (3) and (7), the time derivative of the estimation error is given by:

$$\begin{aligned}\dot{e}_c &= \dot{\bar{x}}_n - \dot{\hat{x}}_{cn} \\ &= A_{\sigma(t)}e_c + \Delta F_{\sigma(t)} - Le_{11} + \bar{d}_{\sigma(t)} \\ &= (A_{\sigma(t)} - Lc)e_c + \Delta F_{\sigma(t)} + \bar{d}_{\sigma(t)},\end{aligned}\quad (9)$$

where

$$A_k = \begin{bmatrix} 0 & h_{\mu1} & 0 & \dots & 0 \\ 0 & 0 & h_{\mu2} & \dots & 0 \\ \vdots & & & \ddots & \\ 0 & \dots & & & h_{\mu,n-1} \\ 0 & \dots & & & 0 \end{bmatrix},$$

and $L = [l_{1k}, \dots, l_{nk}]^T$, $c = [1, 0, \dots, 0]^T$, $\Delta F = [\Delta F_{1k}, \dots, \Delta F_{nk}]^T$, and $\Delta F_{ik} = f_{ik}(\bar{x}_i) - f_{ik}(\hat{x}_{ci})$, with $\bar{d}_k = [d_{1k}, \dots, d_{nk}]^T$.

To assess the stability of the estimation error (8), we define a Lyapunov function $V_{c0} = e_c^T P e_c$, where P is a positive definite matrix to be designed. The derivative of V_{c0} is:

$$\dot{V}_{c0} = 2e_c^T P ((A_k - Lc)e_c + \Delta F_k + \bar{d}_k). \quad (10)$$

Using Assumption 3, we have $\|f_{i\sigma(t)}(\bar{x}_i) - f_{i\sigma(t)}(\hat{x}_{ci})\| \leq q_i \|e_c\|$, where $e_c = \bar{x}_n - \hat{x}_{cn}$. Let $Q = \max_i \{q_i^2\}$. Applying Young's inequality, we obtain:

$$\begin{aligned}2e_c^T P \Delta F_k &\leq e_c^T P^2 e_c + \Delta F_k^T \Delta F_k \\ &\leq e_c^T P^2 e_c + Q e_c^T e_c,\end{aligned}\quad (11)$$

$$\begin{aligned}2e_c^T P \bar{d}_k &\leq \frac{1}{\eta_0} e_c^T P^2 e_c + \eta_0 \bar{d}_k^T \bar{d}_k \\ &\leq \frac{1}{\eta_0} e_c^T P^2 e_c + \eta_0 \|\bar{d}_k\|^2,\end{aligned}\quad (12)$$

where η_0 is a positive constant to be designed. Substituting (10) and (11) into (9), we obtain:

$$\begin{aligned}\dot{V}_{c0} &\leq e_c^T (P(A_k - Lc)) + e_c^T ((A_k - Lc)^T P) \\ &\quad + e_c^T \left(\frac{1 + \eta_0}{\eta_0} P^2 \right) + e_c^T (QI) e_c \\ &\quad + \eta_0 \|\bar{d}_k\|^2\end{aligned}\quad (13)$$

For $i = 0, 1, 2, \dots, n$, the RBF neural network $W_{cik}^T S_{ci}(Z_{ci})$ is used to approximate both the unknown nonlinear function and the control signal $\hat{\alpha}_{cik}(Z_{ci})$ at each step of the process. The constant associated with this approximation is defined as:

$$\theta_{ci} = \max\{\|W_{cik}\|^2 : k \in M\}, \quad (14)$$

where $\hat{\alpha}_{cik}$ and Z_{ci} will be introduced later. Since $\|W_{cik}\|$ is unknown, θ_{ci} is an unknown constant. Define $\tilde{\theta}_{ci} = \theta_{ci} - \hat{\theta}_{ci}$, where $\hat{\theta}_{ci}$ represents the estimate of θ_{ci} .

Building upon these steps, the backstepping technique is employed to derive the actual control law. The design process is structured into n stages. The first $n - 1$ steps focus on formulating the virtual control signal α_{ci} , while the final step (step n) concentrates on determining the actual control input u_k . At each stage, a coordinate transformation is applied to ensure proper design and smooth transition between stages.

Step 1: Define the reference signal y_d and the tracking error $z_{c1} = x_1 - y_d$. Construct the Lyapunov function as:

$$V_{c1k} = \frac{1}{2} z_{c1}^2 + \frac{p_1}{2} \tilde{\theta}_{c1}^2.$$

Differentiating V_{c1k} yields:

$$\begin{aligned}\dot{V}_{c1k} &= z_{c1} \dot{z}_{c1} + p_1 \tilde{\theta}_{c1} \dot{\tilde{\theta}}_{c1} \\ &= z_{c1} (f_{1k} + h_{\mu1} x_2 + d_{1k} - \dot{y}_d) - p_1 \tilde{\theta}_{c1} \dot{\tilde{\theta}}_{c1} \\ &= z_{c1} (f_{1k} + h_{\mu1} \hat{x}_{c2} + h_{\mu1} e_{c2} + d_{1k} - \dot{y}_d) - p_1 \tilde{\theta}_{c1} \dot{\tilde{\theta}}_{c1}.\end{aligned}\quad (15)$$

From Young's inequality [22], we have:

$$z_{c1} h_{\mu1} e_{c2} + z_{c1} d_{1k} \leq \frac{1}{2} e_c^T I_2 e_c + \frac{p_1^2}{2} z_{c1}^2 + \frac{1}{2} z_{c1}^2 + \frac{1}{2} d_{1k}^2. \quad (16)$$

Substituting (15) into (14), we get:

$$\begin{aligned}\dot{V}_{c1k} &\leq z_{c1} \left(f_{1k} + \frac{p_1^2}{2} z_{c1} + \frac{1}{2} z_{c1} - \dot{y}_d + h_{\mu1} \hat{x}_{c2} \right) \\ &\quad + \frac{1}{2} e_c^T I_2 e_c + \frac{1}{2} d_{1k}^2 - p_1 \tilde{\theta}_{c1} \dot{\tilde{\theta}}_{c1} \\ &\leq h_{\mu1} z_{c1} (\hat{x}_{c2} + \bar{f}_{c1k}) + \frac{1}{2} e_c^T I_2 e_c + \frac{1}{2} d_{1k}^2 - p_1 \tilde{\theta}_{c1} \dot{\tilde{\theta}}_{c1},\end{aligned}\quad (17)$$

where $\bar{f}_{c1k}(Z_{c1}) = \frac{1}{h_{\mu1}} \left(f_{1k} + \frac{p_1^2}{2} z_{c1} + \frac{1}{2} z_{c1} - \dot{y}_d \right)$, and $Z_{c1} = [x_1, \hat{\theta}_{c1}, y_d^{(1)}]^T$.

If we choose

$$\hat{\alpha}_{c1k} = -(l_1^c z_{c1} + \bar{f}_{c1k}),$$

where $l_1^c > 0$ is a design parameter, then equation (16) can be rewritten as:

where

$$\begin{aligned} \dot{V}_{c1k} &\leq -l_1^c p_1 z_{c1}^2 + h_{\mu 1} z_{c1} (\hat{x}_{c2} - \hat{\alpha}_{c1k}) + \frac{1}{2} e_c^T I_2 e_c \\ &\quad + \frac{1}{2} d_{1k}^2 - p_1 \tilde{\theta}_{c1} \dot{\hat{\theta}}_{c1}. \end{aligned} \quad (18)$$

Since $\hat{\alpha}_{c1k}$ contains the unknown function f_{c1k} , for any given constant $\varepsilon_{c1} > 0$, we can use the RBF NN $W_{c1k}^T S_{c1}(Z_{c1})$ to approximate $\hat{\alpha}_{c1k}$ as:

$$\begin{aligned} \hat{\alpha}_{c1k} &= W_{c1k}^T S_{c1}(Z_{c1}) + \delta_{c1k}(Z_{c1}), \\ |\delta_{c1k}(Z_{c1})| &\leq \varepsilon_{c1}, \end{aligned} \quad (19)$$

where $\delta_{c1k}(Z_{c1})$ is the approximation error. Consequently, combining (13), (18), and using Young's inequality, we obtain the following inequality:

$$\begin{aligned} -z_{c1} \hat{\alpha}_{c1k} &= -z_{c1} (W_{c1k}^T S_{c1}(Z_{c1}) + \delta_{c1k}(Z_{c1})) \\ &\leq \frac{1}{2a_{c1}^2} z_{c1}^2 \theta_{c1} S_{c1}^T(Z_{c1}) S_{c1}(Z_{c1}) \\ &\quad + \frac{1}{2} z_{c1}^2 + \frac{1}{2} a_{c1}^2 + \frac{1}{2} \varepsilon_{c1}^2, \end{aligned} \quad (20)$$

where $a_{c1} > 0$ is a design parameter.

Next, define the intermediate control signal and update law as:

$$\begin{aligned} \alpha_{c1k} &= -\frac{1}{2a_{c1}^2} z_{c1} \hat{\theta}_{c1} S_{c1}^T(Z_{c1}) S_{c1}(Z_{c1}) \\ \dot{\hat{\theta}}_{c1} &= \frac{1}{2a_{c1}^2} z_{c1}^2 S_{c1}^T(Z_{c1}) S_{c1}(Z_{c1}) - \bar{l}_1^c \hat{\theta}_{c1}, \end{aligned} \quad (21)$$

where $\bar{l}_1^c > 0$ is also a design parameter. Substituting (19) and (20) into (17) yields:

$$\dot{V}_{c1k} \leq \Psi_{c1k} + h_{\mu 1} z_{c1} (\hat{x}_{c2} - \alpha_{c1k}), \quad (22)$$

where $\Psi_{c1k} = -l_1^c p_1 z_{c1}^2 + \frac{p_1}{2} (z_{c1}^2 + a_{c1}^2 + \varepsilon_{c1}^2) + \frac{1}{2} e_c^T I_2 e_c + \frac{1}{2} d_{1k}^2 + p_1 \bar{l}_1^c \hat{\theta}_{c1} \tilde{\theta}_{c1}$.

Step 2: Define

$$z_{c2} = \hat{x}_{c2} - \alpha_{c1k},$$

and consider the following Lyapunov function:

$$V_{c2k} = V_{c1k} + \frac{1}{2} z_{c2}^2 + \frac{p_2}{2} \tilde{\theta}_{c2}^2.$$

The time derivative of V_{c2k} is:

$$\begin{aligned} \dot{V}_{c2k} &= \dot{V}_{c1k} + z_{c2} \dot{z}_{c2} + p_2 \tilde{\theta}_{c2} \dot{\tilde{\theta}}_{c2} \\ &\leq \Psi_{c1k} + h_{\mu 1} z_{c1} z_{c2} + z_{c2} (\dot{\hat{x}}_{c2} - \dot{\alpha}_{c1k}) \\ &\quad - p_2 \tilde{\theta}_{c2} \dot{\hat{\theta}}_{c2} \\ &\leq \Psi_{c1k} + z_{c2} (h_{\mu 1} z_{c1} + f_{2k}(\hat{x}_{c2})) \\ &\quad + z_{c2} (h_{\mu 2} \hat{x}_{c3} + l_{2k} e_{11} - \dot{\alpha}_{c1k}) \\ &\quad - p_2 \tilde{\theta}_{c2} \dot{\hat{\theta}}_{c2}. \end{aligned} \quad (23)$$

$$\begin{aligned} \dot{\alpha}_{c1k} &= \frac{\partial \alpha_{c1k}}{\partial x_1} (f_{1k}(x_1) + h_{\mu 1} (\hat{x}_{c2} + e_{c2}) + d_{1k}) \\ &\quad + \sum_{i=0}^1 \frac{\partial \alpha_{c1k}}{\partial y_d^{(i)}} y_d^{(i+1)} \\ &\quad + \frac{\partial \alpha_{c1k}}{\partial \hat{\theta}_{c1}} \dot{\hat{\theta}}_{c1}. \end{aligned}$$

Using a similar approach as in Step 1, we obtain the following inequality:

$$\begin{aligned} & - \frac{\partial \alpha_{c1k}}{\partial x_1} z_{c2} h_{\mu 1} e_{c2} \\ & - \frac{\partial \alpha_{c1k}}{\partial x_1} z_{c2} d_{1k} \\ & \leq \frac{1}{2} e_c^T I_2 e_c + \frac{1}{2} z_{c2}^2 p_1^2 \left(\frac{\partial \alpha_{c1k}}{\partial x_1} \right)^2 \\ & \quad + \frac{1}{2} z_{c2}^2 \left(\frac{\partial \alpha_{c1k}}{\partial x_1} \right)^2 + \frac{1}{2} d_{1k}^2. \end{aligned} \quad (24)$$

Substituting (22) into (23), we obtain:

$$\begin{aligned} \dot{V}_{c2k} &\leq \Psi_{c1k} + z_{c2} (h_{\mu 1} z_{c1} + f_{2k}(\hat{x}_{c2}) + h_{\mu 2} \hat{x}_{c3} + l_{2k} e_{11}) \\ &\quad - \left(\frac{\partial \alpha_{c1k}}{\partial x_1} (f_{1k}(x_1) + h_{\mu 1} \hat{x}_{c2}) \right. \\ &\quad \left. + \sum_{i=0}^1 \frac{\partial \alpha_{c1k}}{\partial y_d^{(i)}} y_d^{(i+1)} + \frac{\partial \alpha_{c1k}}{\partial \hat{\theta}_{c1}} \dot{\hat{\theta}}_{c1} \right) \\ &\quad + \frac{1}{2} e_c^T I_2 e_c + \frac{1}{2} d_{1k}^2 - p_2 \tilde{\theta}_{c2} \dot{\hat{\theta}}_{c2} \\ &\leq \Psi_{c1k} + z_{c2} (h_{\mu 1} z_{c1} + f_{2k}(\hat{x}_{c2}) + h_{\mu 2} \hat{x}_{c3}) \\ &\quad + \frac{1}{2} e_c^T I_2 e_c + \frac{1}{2} d_{1k}^2 - p_2 \tilde{\theta}_{c2} \dot{\hat{\theta}}_{c2}, \end{aligned} \quad (25)$$

$$Z_{c2} = [x_1, \hat{x}_{c1}, \hat{x}_{c2}, \hat{\theta}_{c1}, y_d^{(2)}]^T, \quad (26)$$

$$\begin{aligned} \bar{f}_{c2k}(Z_{c2}) &= \frac{1}{h_{\mu 2}} (h_{\mu 1} z_{c1} + f_{2k}(\hat{x}_{c2}) + l_{2k} e_{11} \\ &\quad - \frac{\partial \alpha_{c1k}}{\partial x_1} (f_{1k}(x_1) + h_{\mu 1} \hat{x}_{c2}) \\ &\quad - \sum_{i=0}^1 \frac{\partial \alpha_{c1k}}{\partial y_d^{(i)}} y_d^{(i+1)} - \frac{\partial \alpha_{c1k}}{\partial \hat{\theta}_{c1}} \dot{\hat{\theta}}_{c1} \\ &\quad + \frac{1}{2} z_{c2} p_1^2 \left(\frac{\partial \alpha_{c1k}}{\partial x_1} \right)^2 + \frac{1}{2} z_{c2} \left(\frac{\partial \alpha_{c1k}}{\partial x_1} \right)^2). \end{aligned} \quad (27)$$

Finally, following a procedure analogous to Step 1, we define $\hat{\alpha}_{c2k} = -(l_2^c z_{c2} + \bar{f}_{c2k}(Z_{c2}))$, where $l_2^c > 0$ is a design parameter. As a result, equation (24) is updated as:

$$\begin{aligned} \dot{V}_{c2k} &\leq \Psi_{c1k} - l_2^c h_{\mu 2} z_{c2}^2 + h_{\mu 2} z_{c2} (\hat{x}_{c3} - \hat{\alpha}_{c2k}) \\ &\quad + \frac{1}{2} e_c^T I_2 e_c + \frac{1}{2} d_{1k}^2 - p_2 \tilde{\theta}_{c2} \dot{\hat{\theta}}_{c2}. \end{aligned} \quad (28)$$

Furthermore, the RBF neural network $W_{c2k}^T S_{c2}(Z_{c2})$ is used to approximate the unknown nonlinear function $\hat{\alpha}_{c2k}$:

$$\hat{\alpha}_{c2k} = W_{c2k}^T S_{c2}(Z_{c2}) + \delta_{c2k}(Z_{c2}), \quad |\delta_{c2k}(Z_{c2})| \leq \varepsilon_{c2},$$

where $\delta_{c2k}(Z_{c2})$ is the approximation error, and $\varepsilon_{c2} > 0$ is a constant. This leads to the following inequality:

$$\begin{aligned} -z_{c2}\hat{\alpha}_{c2k} &= -z_{c2}(W_{c2k}S_{c2}(Z_{c2}) + \delta_{c2k}(Z_{c2})) \\ &\leq \frac{1}{2a_{c2}^2}z_{c2}^2\theta_{c2}S_{c2}^T(Z_{c2})S_{c2}(Z_{c2}) \\ &\quad + \frac{1}{2}z_{c2}^2 + \frac{1}{2}a_{c2}^2 + \frac{1}{2}\varepsilon_{c2}^2, \end{aligned} \quad (29)$$

where $a_{c2} > 0$ is a design parameter. Now, define the intermediate control signal and update law as:

$$\begin{aligned} \alpha_{c2k} &= -\frac{1}{2a_{c2}^2}z_{c2}\hat{\theta}_{c2}S_{c2}^T(Z_{c2})S_{c2}(Z_{c2}) \\ \dot{\hat{\theta}}_{c2} &= \frac{1}{2a_{c2}^2}z_{c2}^2S_{c2}^T(Z_{c2})S_{c2}(Z_{c2}) - \bar{l}_2^c\hat{\theta}_{c2}, \end{aligned} \quad (30)$$

where $\bar{l}_2^c > 0$ is a design parameter. Combining (25), (26), and (27), we obtain:

$$\dot{V}_{c2k} \leq \Psi_{c2k} + h_{\mu 2}(\hat{x}_{c3} - \alpha_{c2k}), \quad (31)$$

where $\Psi_{c2k} = -\sum_{i=1}^2 l_i^c p_i z_{ci}^2 + \sum_{i=1}^2 \frac{p_i}{2}(z_{ci}^2 + a_{ci}^2 + \varepsilon_{ci}^2) + e_c^T I_2 e_c + d_{1k}^2 + \sum_{i=1}^2 p_i \bar{l}_i^c \hat{\theta}_{ci} \theta_{ci}$.

Step j : At the $(j-1)$ -th step, there exists a Lyapunov function $V_{c,j-1,k}$ such that:

$$\dot{V}_{c,j-1,k} \leq h_{\mu,j-1}z_{c,j-1}(\hat{x}_{c,j} - \alpha_{c,j-1,k}) + \Psi_{c,j-1,k}, \quad (32)$$

and the i -th switched estimator is written as:

$$z_{ci} = \hat{x}_{ci} - \alpha_{c,i-1}(Z_{c,i-1}), \quad i = 2, \dots, j, \quad (33)$$

where $Z_{c,i-1} = [x_1, \hat{x}_{c1}, \dots, \hat{x}_{c,i-1}, \hat{\theta}_{c1}, \dots, \hat{\theta}_{c,i-1}, y_d^{(i-1)}]^T$, and

$$\begin{aligned} \Psi_{c,j-1,k} &= -\sum_{i=1}^{j-1} l_i^c p_i z_{ci}^2 + \sum_{i=1}^{j-1} \frac{p_i}{2}(z_{ci}^2 + a_{ci}^2 + \varepsilon_{ci}^2) \\ &\quad + \frac{j-1}{2}e_c^T I_2 e_c + \frac{j-1}{2}d_{1k}^2 + \sum_{i=1}^{j-1} p_i \bar{l}_i^c \hat{\theta}_{ci} \theta_{ci}. \end{aligned} \quad (34)$$

Continuing the development, at the j -th step, we define the Lyapunov function as follows:

$$V_{cjk} = V_{c,j-1,k} + \frac{1}{2}z_{cj}^2 + \frac{p_j}{2}\tilde{\theta}_{cj}^2. \quad (35)$$

The time derivative of V_{cjk} is then given by:

$$\begin{aligned} \dot{V}_{cjk} &= \dot{V}_{c,j-1,k} + z_{cj}(\dot{\hat{x}}_{cj} - \dot{\alpha}_{c,j-1,k}) - p_j \tilde{\theta}_{cj} \dot{\hat{\theta}}_{cj} \\ &\leq \Psi_{c,j-1,k} + h_{\mu,j-1}z_{c,j-1}z_{cj} \\ &\quad + z_{cj}(f_{jk}(\hat{x}_{cj}) + h_{\mu j}\hat{x}_{c,j+1} + l_{jk}e_{11} - \dot{\alpha}_{c,j-1,k}) \\ &\quad - p_j \tilde{\theta}_{cj} \dot{\hat{\theta}}_{cj}, \end{aligned} \quad (36)$$

where

$$\begin{aligned} \dot{\alpha}_{c,j-1,k} &= \frac{\partial \alpha_{c,j-1,k}}{\partial x_1}(f_{1k} + h_{\mu 1}(\hat{x}_{c2} + e_{c2}) + d_{1k}) \\ &\quad + \sum_{i=1}^{j-1} \frac{\partial \alpha_{c,j-1,k}}{\partial \hat{x}_{ci}} \dot{\hat{x}}_{ci} + \sum_{i=1}^{j-1} \frac{\partial \alpha_{c,j-1,k}}{\partial \hat{\theta}_{ci}} \dot{\hat{\theta}}_{ci} \\ &\quad + \sum_{i=1}^{j-1} \frac{\partial \alpha_{c,j-1,k}}{\partial y_d^{(i)}} y_d^{(i+1)}. \end{aligned}$$

Using a method similar to the one in equation (23) from Step 2, we derive the following inequalities:

$$\begin{aligned} &-z_{cj} \frac{\partial \alpha_{c,j-1,k}}{\partial x_1} h_{\mu 1} e_{c2} - z_{cj} \frac{\partial \alpha_{c,j-1,k}}{\partial x_1} d_{1k} \\ &\leq \frac{1}{2}e_c^T I_2 e_c + \frac{1}{2}z_{cj}^2 p_1^2 \left(\frac{\partial \alpha_{c,j-1,k}}{\partial x_1} \right)^2 \\ &\quad + \frac{1}{2}z_{cj}^2 \left(\frac{\partial \alpha_{c,j-1,k}}{\partial x_1} \right)^2 + \frac{1}{2}d_{1k}^2. \end{aligned} \quad (37)$$

Then, we can express:

$$\begin{aligned} \dot{V}_{cjk} &\leq \Psi_{c,j-1,k} + z_{cj}(\hat{x}_{c,j+1} + \bar{f}_{cjk}(Z_{cj})) + \frac{1}{2}e_c^T I_2 e_c \\ &\quad + \frac{1}{2}d_{1k}^2 - p_j \tilde{\theta}_{cj} \dot{\hat{\theta}}_{cj}, \end{aligned} \quad (38)$$

where

$$\begin{aligned} \bar{f}_{cjk}(Z_{cj}) &= \frac{1}{h_{\mu j}}(h_{\mu,j-1}z_{c,j-1} + f_{jk}(\hat{x}_{cj}) + l_{jk}e_{11} \\ &\quad + \frac{1}{2}z_{cj}p_1^2 \left(\frac{\partial \alpha_{c,j-1,k}}{\partial x_1} \right)^2 + \frac{1}{2}z_{cj} \left(\frac{\partial \alpha_{c,j-1,k}}{\partial x_1} \right)^2 \\ &\quad - \frac{\partial \alpha_{c,j-1,k}}{\partial x_1}(f_{1k} + h_{\mu 1}\hat{x}_{c2}) - \sum_{i=1}^{j-1} \frac{\partial \alpha_{c,j-1,k}}{\partial \hat{x}_{ci}} \dot{\hat{x}}_{ci} \\ &\quad - \sum_{i=1}^{j-1} \frac{\partial \alpha_{c,j-1,k}}{\partial \hat{\theta}_{ci}} \dot{\hat{\theta}}_{ci} - \sum_{i=1}^{j-1} \frac{\partial \alpha_{c,j-1,k}}{\partial y_d^{(i)}} y_d^{(i+1)}). \end{aligned}$$

Thus, by selecting $\hat{\alpha}_{cjk} = -(l_j^c z_{cj} + \bar{f}_{cjk}(Z_{cj}))$, where $l_j^c > 0$ is a design parameter, we obtain:

$$\begin{aligned} \dot{V}_{cjk} &\leq \Psi_{c,j-1,k} - l_j^c h_{\mu j} z_{cj}^2 + h_{\mu j} z_{cj}(\hat{x}_{c,j+1} - \hat{\alpha}_{cjk}) \\ &\quad + \frac{1}{2}e_c^T I_2 e_c + \frac{1}{2}d_{1k}^2 - p_j \tilde{\theta}_{cj} \dot{\hat{\theta}}_{cj}. \end{aligned} \quad (39)$$

Since $\hat{\alpha}_{cjk}$ represents an unknown nonlinear function, we utilize the RBF neural network $W_{cjk}^T S_{cj}(Z_{cj})$ for its approximation. For any constant $\varepsilon_{cj} > 0$, there exists an RBF neural network $W_{cjk}^T S_{cj}(Z_{cj})$ such that:

$$\hat{\alpha}_{cjk} = W_{cjk}^T S_{cj}(Z_{cj}) + \delta_{cj}(Z_{cj}), \quad |\delta_{cj}(Z_{cj})| \leq \varepsilon_{cj}, \quad (40)$$

where $\delta_{cj}(Z_{cj})$ represents the approximation error. From this formulation, we derive the following:

$$\begin{aligned} -z_{cj}\hat{\alpha}_{cjk} &= -z_{cj}(W_{cjk}S_{cj}(Z_{cj}) + \delta_{cj}(Z_{cj})) \\ &\leq \frac{1}{2a_{cj}^2}z_{cj}^2\theta_{cj}S_{cj}^T S_{cj} + \frac{1}{2}z_{cj}^2 + \frac{1}{2}a_{cj}^2 + \frac{1}{2}\varepsilon_{cj}^2, \end{aligned} \quad (41)$$

where $a_{cj} > 0$ is a design parameter. The virtual control signal and update law are defined as:

$$\begin{aligned}\alpha_{cjk}(Z_{cj}) &= -\frac{1}{2a_{cj}^2} z_{cj} \hat{\theta}_{cj} S_{cj}^T S_{cj}, \\ \dot{\hat{\theta}}_{cj} &= \frac{1}{2a_{cj}^2} z_{cj}^2 S_{cj}^T S_{cj} - \bar{l}_j^c \hat{\theta}_{cj},\end{aligned}\quad (42)$$

where $\bar{l}_j^c > 0$ is a design parameter. The following inequalities can be derived from the above formulation:

$$\dot{V}_{cjk} \leq \Psi_{cjk} + h_{\mu j} z_{cj} (\hat{x}_{c,j+1} - \alpha_{cjk}). \quad (43)$$

From the derived formulation, we infer the actual update law as:

$$\begin{aligned}u_{cn} &= \alpha_{cnk}(Z_{cn}) = -\frac{1}{2a_{cn}^2} z_{cn} \hat{\theta}_{cn} S_{cn}^T S_{cn}, \\ \dot{\hat{\theta}}_{cn} &= \frac{1}{2a_{cn}^2} z_{cn}^2 S_{cn}^T S_{cn} - \bar{l}_n^c \hat{\theta}_{cn},\end{aligned}\quad (44)$$

and the corresponding Lyapunov function is given by:

$$\begin{aligned}\dot{V}_{cnk} &\leq \Psi_{c,n-1,k} - l_n^c p_n z_{cn}^2 + \frac{p_n}{2} (z_{cn}^2 + a_{cn}^2 + \varepsilon_{cn}^2) \\ &\quad + \frac{1}{2} e_c I_2 e_c + \frac{1}{2} d_{1k}^2 + p_n \bar{l}_n^c \hat{\theta}_{cn} \tilde{\theta}_{cn}.\end{aligned}\quad (45)$$

We define the overall Lyapunov function as:

$$V_{ck} = e_c^T P e_c + V_{cnk}.$$

By combining equations (13) and (43), the derivative of V_{ck} satisfies the following inequality:

$$\begin{aligned}\dot{V}_{ck} &\leq e_c^T \Lambda_c e_c - \sum_{i=1}^n l_i^c p_i z_{ci}^2 + \sum_{i=1}^n \frac{p_i}{2} (z_{ci}^2 + a_{ci}^2 + \varepsilon_{ci}^2) \\ &\quad + \frac{n}{2} d_{1k}^2 + \sum_{i=1}^n p_i \bar{l}_i^c \hat{\theta}_{ci} \tilde{\theta}_{ci} + \eta_0 \|\bar{d}_k\|^2,\end{aligned}\quad (46)$$

where $\Lambda_c = P(A_k - Lc) + (A_k - Lc)^T P + \frac{1+\eta_0}{\eta_0} PP + QI + \frac{n}{2} I_2$.

B. State Estimator and Backstepping Control Design Under Data-Loss Conditions

In the case where data loss occurs due to transmission issues, the received data becomes unreliable. Rather than discarding it, we propose using previous valid data as a substitute for the current data. In this case, the relation $x_1 \neq y$ holds. Let the estimation errors be defined as $e_{si} = x_i - \hat{x}_{si}$, $i = 1, 2, \dots, n$, where $e'_{s1} = x'_1 - \hat{x}_{s1}$ and $\Delta e_1 = e_{s1} - e'_{s1} = x_1 - x'_1$. Here, \hat{x}_{si} represents the estimated state variables, and x'_1 denotes the last valid observation. The switched estimator in the presence of data loss is designed as follows:

$$\begin{aligned}\dot{\hat{x}}_{s1} &= f_{1\sigma(t)}(\hat{x}_{s1}) + h_{\mu 1} \hat{x}_{s2} + l_{1\sigma(t)}(x'_1 - \hat{x}_{s1}) \\ &\vdots \\ \dot{\hat{x}}_{si} &= f_{i\sigma(t)}(\hat{x}_{si}) + h_{\mu i} \hat{x}_{s,i+1} + l_{i\sigma(t)}(x'_1 - \hat{x}_{s1}) \\ \dot{\hat{x}}_{sn} &= f_{n\sigma(t)}(\hat{x}_{sn}) + h_{\mu n} u + l_{n\sigma(t)}(x'_1 - \hat{x}_{s1}),\end{aligned}\quad (47)$$

Let $e_s = \bar{x}_n - \hat{x}_{sn}$ denote the estimator error in this case. Based on equations (3) and (44), the time derivative of the estimation error is:

$$\begin{aligned}\dot{e}_s &= \dot{\bar{x}}_n - \dot{\hat{x}}_{sn} \\ &= A_{\sigma(t)} e_s + \Delta F_{\sigma(t)} - L e'_{s1} + \bar{d}_{\sigma(t)} \\ &= (A_{\sigma(t)} - Lc) e_s + \Delta F_{\sigma(t)} + \bar{d}_{\sigma(t)},\end{aligned}\quad (48)$$

where

$$A_k = \begin{bmatrix} 0 & h_{\mu 1} & 0 & \dots & 0 \\ 0 & 0 & h_{\mu 2} & \dots & 0 \\ \vdots & & & \ddots & \\ 0 & \dots & & & h_{\mu, n-1} \\ 0 & \dots & & & 0 \end{bmatrix},$$

$L = [l_{1k}, \dots, l_{nk}]^T$, $c = [1, 0, \dots, 0]$, $\Delta F = [\Delta F_{1k}, \dots, \Delta F_{nk}]^T$, where $\Delta F_{ik} = f_{ik}(\bar{x}_i) - f_{ik}(\hat{x}_{si})$, and $\bar{d}_k = [d_{1k}, \dots, d_{nk}]^T$.

Assumption 3.1: There exists a known constant h , such that the following inequality holds:

$$|\Delta e_{s1}| \leq h. \quad (49)$$

To investigate the stability of the estimator error \dot{e}_s , we define a Lyapunov function candidate $V_{sc0} = e_s^T P e_s$, where P is a positive definite matrix to be designed. The time derivative of V_{s0} is:

$$\dot{V}_{s0} = 2e_s^T P ((A_k - Lc)e_s + L\Delta e_{s1} + \Delta F_k + \bar{d}_k). \quad (50)$$

Using Assumption 3, we can derive the inequality $\|f_{i\sigma(t)}(\bar{x}_i) - f_{i\sigma(t)}(\hat{x}_{si})\| \leq q_i \|e_s\|$, where $e_s = \bar{x}_n - \hat{x}_{sn}$. Let $Q = \max_i \{q_i^2\}$, and by applying Young's inequality, we obtain:

$$\begin{aligned}2e_s^T P \Delta F_k &\leq e_s^T P P e_s + \Delta F_k^T \Delta F_k \\ &\leq e_s^T P P e_s + Q e_s^T e_s,\end{aligned}\quad (51)$$

$$\begin{aligned}2e_s^T P \bar{d}_k &\leq \frac{1}{\eta_1} e_s^T P P e_s + \eta_1 \bar{d}_k^T \bar{d}_k \\ &\leq \frac{1}{\eta_1} e_s^T P P e_s + \eta_1 \|\bar{d}_k\|^2,\end{aligned}\quad (52)$$

$$2e_s^T P L \Delta e_{s1} \leq \frac{1}{\eta_2} e_s^T P L L^T P e_s + \eta_2 h^2, \quad (53)$$

where η_1 and η_2 are positive constant parameters to be chosen. Substituting equations (48), (49), and (50) into (47) results in:

$$\begin{aligned}\dot{V}_{s0} &\leq e_s^T \left(P(A_k - Lc) + (A_k - Lc)^T P + \frac{1+\eta_1}{\eta_1} PP \right. \\ &\quad \left. + \frac{1}{\eta_2} P L L^T P + QI \right) e_s + \eta_1 \|\bar{d}_k\|^2 + \eta_2 h^2.\end{aligned}\quad (54)$$

Next, the RBF neural network $W_{sik}^T S_{si}(Z_{si})$ is used to approximate the unknown nonlinear function and control signal $\hat{\alpha}_{sik}(Z_{si})$. We define the constant as:

$$\theta_{si} = \max \{ \|W_{sik}\|^2 : k \in M \}, \quad i = 0, 1, 2, \dots, n, \quad (55)$$

where the functions $\hat{\alpha}_{sik}$ and the vector Z_{si} are specified at each step. Since $\|W_{sik}\|$ is unknown, θ_{si} remains an unknown constant. We define the error term $\tilde{\theta}_{si} = \theta_{si} - \hat{\theta}_{si}$, where $\tilde{\theta}_{si}$ represents the estimate of θ_{si} .

Step 1: Design $z_{s1} = x_1 - y_d$ and construct the Lyapunov function as:

$$V_{s1k} = \frac{1}{2}z_{s1}^2 + \frac{p_1}{2}\tilde{\theta}_{s1}^2.$$

Differentiating V_{s1k} yields:

$$\begin{aligned} \dot{V}_{s1k} &= z_{s1}\dot{z}_{s1} + p_1\tilde{\theta}_{s1}\dot{\tilde{\theta}}_{s1} \\ &= z_{s1}(f_{1k}(x_1) + h_{\mu 1}x_2 + d_{1k} - \dot{y}_d) \\ &\quad - p_1\tilde{\theta}_{s1}\dot{\tilde{\theta}}_{s1} \\ &= z_{s1}(f_{1k}(x_1) + f_{1k}(\hat{x}_{s1}) - f_{1k}(\hat{x}_{s1}) \\ &\quad + h_{\mu 1}(\hat{x}_{s2} + e_{s2}) + d_{1k} - \dot{y}_d) \\ &\quad - p_1\tilde{\theta}_{s1}\dot{\tilde{\theta}}_{s1}. \end{aligned} \quad (56)$$

From Young's inequality:

$$\begin{aligned} z_{s1}(f_{1k}(x_1) - f_{1k}(\hat{x}_{s1})) &\leq \frac{1}{2}z_{s1}^2 \\ &\quad + \frac{1}{2}q_1^2e_s^T I_1 e_s \\ z_{s1}h_{\mu 1}e_{s2} + z_{s1}d_{1k} &\leq \frac{1}{2}e_s^T I_2 e_s \\ &\quad + \frac{p_1^2}{2}z_{s1}^2 + \frac{1}{2}z_{s1}^2 \\ &\quad + \frac{1}{2}d_{1k}^2. \end{aligned} \quad (57)$$

Substituting (54) into (53), we obtain:

$$\begin{aligned} \dot{V}_{s1k} &\leq z_{s1}\left(f_{1k}(\hat{x}_{s1}) + h_{\mu 1}\hat{x}_{s2}\right. \\ &\quad \left.+ \frac{p_1^2}{2}z_{s1} + \frac{1}{2}z_{s1} + \frac{1}{2}z_{s1} - \dot{y}_d\right) \\ &\quad + \frac{1}{2}q_1^2e_s^T I_1 e_s + \frac{1}{2}e_s^T I_2 e_s \\ &\quad + \frac{1}{2}d_{1k}^2 - p_1\tilde{\theta}_{s1}\dot{\tilde{\theta}}_{s1} \\ &\leq h_{\mu 1}z_{s1}(\hat{x}_{s2} + \bar{f}_{s1k}) \\ &\quad + \frac{1}{2}q_1^2e_s^T I_1 e_s + \frac{1}{2}e_s^T I_2 e_s \\ &\quad + \frac{1}{2}d_{1k}^2 - p_1\tilde{\theta}_{s1}\dot{\tilde{\theta}}_{s1}. \end{aligned} \quad (58)$$

where

$$\bar{f}_{s1k}(Z_{s1}) = \frac{1}{h_{\mu 1}}\left(f_{1k} + \frac{p_1^2}{2}z_{s1} + z_{s1} - \dot{y}_d\right),$$

and $Z_{s1} = [x_1, \hat{\theta}_{s1}, \bar{y}_d^{(1)}]^T$.

If we choose

$$\hat{\alpha}_{s1k} = -(l_1^s z_{s1} + \bar{f}_{s1k}),$$

where $l_1^s > 0$ is a design parameter, then (55) can be changed into the following form

$$\begin{aligned} \dot{V}_{s1k} &\leq -l_1^s p_1 z_{s1}^2 + h_{\mu 1} z_{s1}(\hat{x}_{s2} - \hat{\alpha}_{s1k}) + \frac{1}{2}e_s^T I_2 e_s \\ &\quad + \frac{1}{2}q_1^2e_s^T I_1 e_s + \frac{1}{2}d_{1k}^2 - p_1\tilde{\theta}_{s1}\dot{\tilde{\theta}}_{s1}. \end{aligned} \quad (59)$$

Since $\hat{\alpha}_{s1k}$ contains the unknown term f_{s1k} , it is approximated using an RBF NN of the form $W_{s1k}^\top S_{s1}(Z_{s1})$. For any constant $\varepsilon_{s1} > 0$, this yields:

$$\hat{\alpha}_{s1k} = W_{s1k}^\top S_{s1}(Z_{s1}) + \delta_{s1k}(Z_{s1}), \quad |\delta_{s1k}(Z_{s1})| \leq \varepsilon_{s1}, \quad (60)$$

where $\delta_{s1k}(Z_{s1})$ denotes the approximation error bounded by ε_{s1} . By applying (13), (57), and Young's inequality, we have:

$$\begin{aligned} -z_{s1}\hat{\alpha}_{s1k} &= -z_{s1}(W_{s1k}^\top S_{s1}(Z_{s1}) + \delta_{s1k}(Z_{s1})) \\ &\leq \frac{z_{s1}^2}{2a_{s1}^2}\theta_{s1}^\top S_{s1}^\top(Z_{s1})S_{s1}(Z_{s1}) \\ &\quad + \frac{1}{2}z_{s1}^2 + \frac{1}{2}a_{s1}^2 + \frac{1}{2}\varepsilon_{s1}^2, \end{aligned} \quad (61)$$

where $a_{s1} > 0$ is a design parameter chosen to ensure stability.

We define the intermediate control signal and update law as:

$$\begin{aligned} \alpha_{s1k} &= -\frac{1}{2a_{s1}^2}(x'_1 - y_d)\hat{\theta}_{s1}S_{s1}^\top(Z_{s1})S_{s1}(Z_{s1}), \\ \dot{\hat{\theta}}_{s1} &= \frac{1}{2a_{s1}^2}(x'_1 - y_d)^2 S_{s1}^\top(Z_{s1})S_{s1}(Z_{s1}) - \bar{l}_1^s \hat{\theta}_{s1}, \end{aligned} \quad (62)$$

where $\bar{l}_1^s > 0$ is another design parameter.

Substituting (58) and (59) into equation (56) yields:

$$\dot{V}_{s1k} \leq \Psi_{s1k} + h_{\mu 1} z_{s1}(\hat{x}_{s2} - \alpha_{s1k}), \quad (63)$$

where:

$$\begin{aligned} \Psi_{s1k} &= -l_1^s p_1 z_{s1}^2 + \frac{p_1}{2}(z_{s1}^2 + a_{s1}^2 + \varepsilon_{s1}^2) \\ &\quad + \frac{1}{2}q_1^2e_s^T I_1 e_s + \frac{1}{2}e_s^T I_2 e_s + \frac{1}{2}d_{1k}^2 \\ &\quad + p_1\bar{l}_1^s \hat{\theta}_{s1}\tilde{\theta}_{s1} \\ &\quad + \frac{p_1}{4a_{s1}^2}h\tilde{\theta}_{s1}l^s((x'_1)^2 + y_d^2). \end{aligned}$$

Step 2: Define

$$z_{s2} = \hat{x}_{s2} - \alpha_{s1k},$$

and consider the Lyapunov function:

$$V_{s2k} = V_{s1k} + \frac{1}{2}z_{s2}^2 + \frac{p_2}{2}\tilde{\theta}_{s2}^2.$$

The time derivative of V_{s2k} is given by:

$$\begin{aligned} \dot{V}_{s2k} &= \dot{V}_{s1k} + z_{s2}\dot{z}_{s2} + p_2\tilde{\theta}_{s2}\dot{\tilde{\theta}}_{s2} \\ &\leq \Psi_{s1k} + h_{\mu 1} z_{s1} z_{s2} + z_{s2}(\dot{\hat{x}}_{s2} - \dot{\alpha}_{s1k}) \\ &\quad - p_2\tilde{\theta}_{s2}\dot{\tilde{\theta}}_{s2} \\ &\leq \Psi_{s1k} + z_{s2}(h_{\mu 1} z_{s1} + f_{2k}(\hat{x}_{s2}) + h_{\mu 2}\hat{x}_{s3} + l_{2k}e'_{s1} \\ &\quad - \dot{\alpha}_{s1k}) - p_2\tilde{\theta}_{s2}\dot{\tilde{\theta}}_{s2}. \end{aligned} \quad (64)$$

where $\dot{\alpha}_{s1k}$ is given by:

$$\begin{aligned}\dot{\alpha}_{s1k} = & \frac{\partial \alpha_{s1k}}{\partial x_1} (f_{1k}(x_1) + h_{\mu 1}(\hat{x}_{s2} + e_{s2}) + d_{1k}) \\ & + \sum_{i=0}^1 \frac{\partial \alpha_{s1k}}{\partial y_d^{(i)}} y_d^{(i+1)} + \frac{\partial \alpha_{s1k}}{\partial \hat{\theta}_{s1}} \dot{\theta}_{s1}.\end{aligned}$$

Using the completion of squares method, we obtain the following inequality:

$$\begin{aligned}& -\frac{\partial \alpha_{s1k}}{\partial x_1} z_{s2} h_{\mu 1} e_{s2} - \frac{\partial \alpha_{s1k}}{\partial x_1} z_{s2} d_{1k} \\ & \leq \frac{1}{2} e_s^T I_2 e_s + \frac{1}{2} z_{s2}^2 p_1^2 \left(\frac{\partial \alpha_{s1k}}{\partial x_1} \right)^2 \\ & \quad + \frac{1}{2} z_{s2}^2 \left(\frac{\partial \alpha_{s1k}}{\partial x_1} \right)^2 + \frac{1}{2} d_{1k}^2.\end{aligned}\quad (65)$$

Substituting (62) into (63), we get:

$$\begin{aligned}\dot{V}_{s2k} \leq & \Psi_{s1k} \\ & + z_{s2} \left(h_{\mu 1} z_{s1} + f_{2k}(\hat{x}_{s2}) \right. \\ & \left. + h_{\mu 2} \hat{x}_{s3} + l_{2k} e'_{s1} - \dot{\alpha}_{s1k} \right) \\ & - \left(\frac{\partial \alpha_{s1k}}{\partial x_1} (f_{1k}(x_1) + h_{\mu 1} \hat{x}_{s2}) \right. \\ & \left. + \sum_{i=0}^1 \frac{\partial \alpha_{s1k}}{\partial y_d^{(i)}} y_d^{(i+1)} + \frac{\partial \alpha_{s1k}}{\partial \hat{\theta}_{s1}} \dot{\theta}_{s1} \right) \\ & + \frac{1}{2} z_{s2}^2 p_1^2 \left(\frac{\partial \alpha_{s1k}}{\partial x_1} \right)^2 + \frac{1}{2} z_{s2}^2 \left(\frac{\partial \alpha_{s1k}}{\partial x_1} \right)^2 \\ & + \frac{1}{2} e_s^T I_2 e_s + \frac{1}{2} d_{1k}^2 - p_2 \tilde{\theta}_{s2} \dot{\theta}_{s2} \\ & \leq \Psi_{s1k} + h_{\mu 2} z_{s2} (\bar{f}_{s2k}(Z_{s2}) + \hat{x}_{s3}) \\ & + \frac{1}{2} e_s^T I_2 e_s + \frac{1}{2} d_{1k}^2 - p_2 \tilde{\theta}_{s2} \dot{\theta}_{s2}.\end{aligned}\quad (66)$$

where $Z_{s2} = [x_1, \hat{x}_{s1}, \hat{x}_{s2}, \hat{\theta}_{s1}, \bar{y}_d^{(2)}]^T$, and $\bar{f}_{s2k}(Z_{s2})$ is defined as:

$$\begin{aligned}\bar{f}_{s2k}(Z_{s2}) = & \frac{1}{h_{\mu 2}} \left(h_{\mu 1} z_{s1} + f_{2k}(\hat{x}_{s2}) \right. \\ & \left. + l_{2k} e'_{s1} - \frac{\partial \alpha_{s1k}}{\partial x_1} (f_{1k}(x_1) + h_{\mu 1} \hat{x}_{s2}) \right. \\ & \left. - \sum_{i=0}^1 \frac{\partial \alpha_{s1k}}{\partial y_d^{(i)}} y_d^{(i+1)} - \frac{\partial \alpha_{s1k}}{\partial \hat{\theta}_{s1}} \dot{\theta}_{s1} \right. \\ & \left. + \frac{1}{2} z_{s2}^2 p_1^2 \left(\frac{\partial \alpha_{s1k}}{\partial x_1} \right)^2 + \frac{1}{2} z_{s2}^2 \left(\frac{\partial \alpha_{s1k}}{\partial x_1} \right)^2 \right).\end{aligned}$$

Finally, by selecting $\hat{\alpha}_{s2k} = -(l_2^s z_{s2} + \bar{f}_{s2k}(Z_{s2}))$, where $l_2^s > 0$ is a design parameter, equation (64) simplifies to:

$$\begin{aligned}\dot{V}_{s2k} \leq & \Psi_{s1k} - l_2^s h_{\mu 2} z_{s2}^2 + h_{\mu 2} z_{s2} (\hat{x}_{s3} - \hat{\alpha}_{s2k}) \\ & + \frac{1}{2} e_s^T I_2 e_s + \frac{1}{2} d_{1k}^2 - p_2 \tilde{\theta}_{s2} \dot{\theta}_{s2}.\end{aligned}\quad (67)$$

By completing the square, the following inequality is obtained:

$$\begin{aligned}& -\frac{\partial \alpha_{s1k}}{\partial x_1} z_{s2} h_{\mu 1} e_{s2} - \frac{\partial \alpha_{s1k}}{\partial x_1} z_{s2} d_{1k} \leq \frac{1}{2} e_s^T I_2 e_s \\ & \quad + \frac{1}{2} z_{s2}^2 p_1^2 \left(\frac{\partial \alpha_{s1k}}{\partial x_1} \right)^2 \\ & \quad + \frac{1}{2} z_{s2}^2 \left(\frac{\partial \alpha_{s1k}}{\partial x_1} \right)^2 \\ & \quad + \frac{1}{2} d_{1k}^2.\end{aligned}\quad (68)$$

Substituting (62) into (63) leads to the following:

$$\begin{aligned}\dot{V}_{s2k} \leq & \Psi_{s1k} + z_{s2} (h_{\mu 1} z_{s1} + f_{2k}(\hat{x}_{s2}) + h_{\mu 2} \hat{x}_{s3} + l_{2k} e'_{s1}) \\ & - \left(\frac{\partial \alpha_{s1k}}{\partial x_1} (f_{1k}(x_1) + h_{\mu 1} \hat{x}_{s2}) + \sum_{i=0}^1 \frac{\partial \alpha_{s1k}}{\partial y_d^{(i)}} y_d^{(i+1)} \right. \\ & \left. + \frac{\partial \alpha_{s1k}}{\partial \hat{\theta}_{s1}} \dot{\theta}_{s1} + \frac{1}{2} z_{s2}^2 p_1^2 \left(\frac{\partial \alpha_{s1k}}{\partial x_1} \right)^2 + \frac{1}{2} z_{s2}^2 \left(\frac{\partial \alpha_{s1k}}{\partial x_1} \right)^2 \right) \\ & + \frac{1}{2} e_s^T I_2 e_s + \frac{1}{2} d_{1k}^2 - p_2 \tilde{\theta}_{s2} \dot{\theta}_{s2} \\ & \leq \Psi_{s1k} + h_{\mu 2} z_{s2} (\bar{f}_{s2k}(Z_{s2}) + \hat{x}_{s3}) \\ & + \frac{1}{2} e_s^T I_2 e_s + \frac{1}{2} d_{1k}^2 - p_2 \tilde{\theta}_{s2} \dot{\theta}_{s2},\end{aligned}\quad (69)$$

where:

$$Z_{s2} = [x_1, \hat{x}_{s1}, \hat{x}_{s2}, \hat{\theta}_{s1}, \bar{y}_d^{(2)}]^T,$$

and

$$\begin{aligned}\bar{f}_{s2k}(Z_{s2}) = & \frac{1}{h_{\mu 2}} (h_{\mu 1} z_{s1} + f_{2k}(\hat{x}_{s2}) + l_{2k} e'_{s1}) \\ & - \frac{\partial \alpha_{s1k}}{\partial x_1} (f_{1k}(x_1) + h_{\mu 1} \hat{x}_{s2}) \\ & - \sum_{i=0}^1 \frac{\partial \alpha_{s1k}}{\partial y_d^{(i)}} y_d^{(i+1)} - \frac{\partial \alpha_{s1k}}{\partial \hat{\theta}_{s1}} \dot{\theta}_{s1} \\ & + \frac{1}{2} z_{s2}^2 p_1^2 \left(\frac{\partial \alpha_{s1k}}{\partial x_1} \right)^2 + \frac{1}{2} z_{s2}^2 \left(\frac{\partial \alpha_{s1k}}{\partial x_1} \right)^2.\end{aligned}$$

If we choose $\hat{\alpha}_{s2k} = -(l_2^s z_{s2} + \bar{f}_{s2k}(Z_{s2}))$, where $l_2^s > 0$ is a design parameter, equation (64) simplifies to:

$$\begin{aligned}\dot{V}_{s2k} \leq & \Psi_{s1k} - l_2^s h_{\mu 2} z_{s2}^2 + h_{\mu 2} z_{s2} (\hat{x}_{s3} - \hat{\alpha}_{s2k}) \\ & + \frac{1}{2} e_s^T I_2 e_s + \frac{1}{2} d_{1k}^2 - p_2 \tilde{\theta}_{s2} \dot{\theta}_{s2}.\end{aligned}\quad (70)$$

Furthermore, we use the RBF NN $W_{s2k}^T S_{s2}(Z_{s2})$ to approximate the unknown nonlinear function $\hat{\alpha}_{s2k}$:

$$\hat{\alpha}_{s2k} = W_{s2k}^T S_{s2}(Z_{s2}) + \delta_{s2k}(Z_{s2}), \quad |\delta_{s2k}(Z_{s2})| \leq \varepsilon_{s2},$$

where $\delta_{s2k}(Z_{s2})$ is the approximation error, and $\varepsilon_{s2} > 0$ is a constant. Substituting this approximation into the previous equations:

$$\begin{aligned}-z_{s2} \hat{\alpha}_{s2k} = & -z_{s2} (W_{s2k}^T S_{s2}(Z_{s2}) + \delta_{s2k}(Z_{s2})) \\ & \leq \frac{1}{2a_{s2}^2} z_{s2}^2 \theta_{s2} S_{s2}^T(Z_{s2}) S_{s2}(Z_{s2}) \\ & \quad + \frac{1}{2} z_{s2}^2 + \frac{1}{2} a_{s2}^2 + \frac{1}{2} \varepsilon_{s2}^2,\end{aligned}\quad (71)$$

where $a_{s2} > 0$ is a design parameter. The intermediate control signal and update law are constructed as:

$$\begin{aligned}\alpha_{s2k} &= -\frac{1}{2a_{s2}^2} z_{s2} \hat{\theta}_{s2} S_{s2}^T(Z_{s2}) S_{s2}(Z_{s2}), \\ \dot{\hat{\theta}}_{s2} &= \frac{1}{2a_{s2}^2} z_{s2}^2 S_{s2}^T(Z_{s2}) S_{s2}(Z_{s2}) - \bar{l}_2^s \hat{\theta}_{s2}.\end{aligned}\quad (72)$$

Substituting these into equations (45)-(47), we obtain:

$$\dot{V}_{s2k} \leq \Psi_{s2k} + h_{\mu2}(\hat{x}_{s3} - \alpha_{s2k}), \quad (73)$$

where Ψ_{s2k} is given by:

$$\begin{aligned}\Psi_{s2k} &= -\sum_{i=1}^2 l_i^s p_i z_{si}^2 + \sum_{i=1}^2 \frac{p_i}{2} (z_{si}^2 + a_{si}^2 + \varepsilon_{si}^2) \\ &\quad + e_s^T I_2 e_s + d_{1k}^2 + \sum_{i=1}^2 p_i \bar{l}_i^s \hat{\theta}_{si} \tilde{\theta}_{si} \\ &\quad + \frac{1}{2} q_1^2 e_s^T I_1 e_s + \frac{p_1}{4a_{s1}^2} h l^s \tilde{\theta}_{s1} ((x'_1)^2 + y_d^2).\end{aligned}$$

For step j , we define the Lyapunov function:

$$V_{sjk} = V_{s,j-1,k} + \frac{1}{2} z_{sj}^2 + \frac{p_j}{2} \tilde{\theta}_{sj}^2.$$

Further, the RBF NN $W_{s2k}^T S_{s2}(Z_{s2})$ is used to approximate the unknown nonlinear function $\hat{\alpha}_{s2k}$.

$$\hat{\alpha}_{s2k} = W_{s2k}^T S_{s2}(Z_{s2}) + \delta_{s2k}(Z_{s2}), |\delta_{s2k}(Z_{s2})| \leq \varepsilon_{s2},$$

where $\delta_{s2k}(Z_{s2})$ is the approximation error, and $\varepsilon_{s2} > 0$ is an arbitrary constant. Then, a simple calculation yields

$$\begin{aligned}-z_{s2} \hat{\alpha}_{s2k} &= -z_{s2} (W_{s2k} S_{s2}(Z_{s2}) + \delta_{s2k}(Z_{s2})) \\ &\leq \frac{1}{2a_{s2}^2} z_{s2}^2 \theta_{s2} S_{s2}^T(Z_{s2}) S_{s2}(Z_{s2}) \\ &\quad + \frac{1}{2} z_{s2}^2 + \frac{1}{2} a_{s2}^2 + \frac{1}{2} \varepsilon_{s2}^2,\end{aligned}\quad (74)$$

where $a_{s2} > 0$ is a design parameter. Now, construct the intermediate control signal and update law as

$$\begin{aligned}\alpha_{s2k} &= -\frac{1}{2a_{s2}^2} z_{s2} \hat{\theta}_{s2} S_{s2}^T(Z_{s2}) S_{s2}(Z_{s2}) \\ \dot{\hat{\theta}}_{s2} &= \frac{1}{2a_{s2}^2} z_{s2}^2 S_{s2}^T(Z_{s2}) S_{s2}(Z_{s2}) - \bar{l}_2^s \hat{\theta}_{s2},\end{aligned}\quad (75)$$

where $\bar{l}_2^s > 0$ is also a design parameter. Putting together (45)-(47) gives

$$\dot{V}_{s2k} \leq \Psi_{s2k} + h_{\mu2}(\hat{x}_{s3} - \alpha_{s2k}), \quad (76)$$

where $\Psi_{s2k} = -\sum_{i=1}^2 l_i^s p_i z_{si}^2 + \sum_{i=1}^2 \frac{p_i}{2} (z_{si}^2 + a_{si}^2 + \varepsilon_{si}^2) + e_s^T I_2 e_s + d_{1k}^2 + \sum_{i=1}^2 p_i \bar{l}_i^s \hat{\theta}_{si} \tilde{\theta}_{si} + \frac{1}{2} q_1^2 e_s^T I_1 e_s + \frac{p_1}{4a_{s1}^2} h l^s \tilde{\theta}_{s1} ((x'_1)^2 + y_d^2).$

Step j : At the $(j-1)$ th step, there exist a Lyapunov function $V_{s,j-1,k}$ that

$$V_{s,j-1,k} \leq h_{\mu,j-1} z_{s,j-1}(\hat{x}_{sj} - \alpha_{s,j-1,k}) + \Psi_{s,j-1,k}, \quad (77)$$

and the i th switched estimator can be written that

$$z_{si} = \hat{x}_{si} - \alpha_{s,i-1}(Z_{s,i-1}), \quad i = 2, \dots, j, \quad (78)$$

where $Z_{s,i-1} = [x_1, \hat{x}_{s1}, \dots, \hat{x}_{s,i-1}, \hat{\theta}_{s1}, \dots, \hat{\theta}_{s,i-1}, \bar{y}_d^{(i-1)}]^T$, and

$$\begin{aligned}\Psi_{s,j-1,k} &= -\sum_{i=1}^{j-1} l_i^s p_i z_{si}^2 + \sum_{i=1}^{j-1} \frac{p_i}{2} (z_{si}^2 + a_{si}^2 + \varepsilon_{si}^2) \\ &\quad + \frac{j-1}{2} e_s^T I_2 e_s + \frac{j-1}{2} d_{1k}^2 + \sum_{i=1}^{j-1} p_i \bar{l}_i^s \hat{\theta}_{si} \tilde{\theta}_{si} \\ &\quad + \frac{1}{2} q_1^2 e_s^T I_1 e_s + \frac{p_1}{4a_{s1}^2} h l^s \tilde{\theta}_{s1} ((x'_1)^2 + y_d^2).\end{aligned}\quad (79)$$

Continuing to promote, at the j th step, define the following Lyapunov function as

$$V_{sjk} = V_{s,j-1,k} + \frac{1}{2} z_{sj}^2 + \frac{p_j}{2} \tilde{\theta}_{sj}^2. \quad (80)$$

Since the RBF NN approximation is used, this step follows the same reasoning as in the standard case to reach the result.

Here, $a_{sj} > 0$ is a design parameter. The virtual control input and its adaptation law are given by:

$$\begin{aligned}\alpha_{sjk}(Z_{sj}) &= -\frac{1}{2a_{sj}^2} z_{sj} \hat{\theta}_{sj} S_{sj}^T S_{sj}, \\ \dot{\hat{\theta}}_{sj} &= \frac{1}{2a_{sj}^2} z_{sj}^2 S_{sj}^T S_{sj} - \bar{l}_j^s \hat{\theta}_{sj},\end{aligned}\quad (81)$$

where $\bar{l}_j^s > 0$ is a selected design parameter.

This completes the induction. At Step n , a unified output-feedback controller can be applied to all subsystems with the update rule:

$$\begin{aligned}u_{sk} &= \alpha_{snk}(Z_{sn}) = -\frac{1}{2a_{sn}^2} z_{sn} \hat{\theta}_{cn} S_{sn}^T S_{sn}, \\ \dot{\hat{\theta}}_{sn} &= \frac{1}{2a_{sn}^2} z_{sn}^2 S_{sn}^T S_{sn} - \bar{l}_n^s \hat{\theta}_{sn},\end{aligned}\quad (82)$$

and the Lyapunov function derivative satisfies:

$$\begin{aligned}\dot{V}_{snk} &\leq \Psi_{s,n-1,k} - l_n^s p_n z_{sn}^2 + \frac{p_n}{2} (z_{sn}^2 + a_{sn}^2 + \varepsilon_{sn}^2) \\ &\quad + \frac{1}{2} e_s^T I_2 e_s + \frac{1}{2} d_{1k}^2 + p_n \bar{l}_n^s \hat{\theta}_{sn} \tilde{\theta}_{sn}.\end{aligned}\quad (83)$$

Define the overall Lyapunov function as:

$$V_{sk} = e_s^T P e_s + V_{snk}.$$

By combining equations (52) and (75), the derivative of V_{ck} is expressed as:

$$\begin{aligned}\dot{V}_{sk} &\leq e_s^T \Lambda_s e_s - \sum_{i=1}^n l_i^s p_i z_{si}^2 + \sum_{i=1}^n \frac{p_i}{2} (z_{si}^2 + a_{si}^2 + \varepsilon_{si}^2) \\ &\quad + \frac{n}{2} d_{1k}^2 + \sum_{i=1}^n p_i \bar{l}_i^s \hat{\theta}_{si} \tilde{\theta}_{si} + \eta_1 \|\bar{d}_k\|^2 \\ &\quad + \eta_2 h^2 + \frac{p_1}{4a_{s1}^2} h l^s \tilde{\theta}_{s1} ((x'_1)^2 + y_d^2),\end{aligned}\quad (84)$$

where $\Lambda_s = P(A_k - Lc) + (A_k - Lc)^T P + \frac{1+\eta_1}{\eta_1} PP + \frac{1}{\eta_2} PLL^T P + QI + \frac{q_1^2}{2} I_1 + \frac{n}{2} I_2.$

In this work, we introduce distinct update laws (42) and (72) for the different subsystems, providing practical advantages in their application.

C. Stability Analysis

This section addresses the boundedness of all signals within the closed-loop system, both for ideal and imperfect measurements. The initial parameters are specified as follows:

$$a_{c0} = \min_{k \in M} \left\{ \frac{\lambda_{\min}(\Lambda'_c) - \frac{n}{2}}{\lambda_{\max}(P)} \right\} \\ l_i^c - \frac{p_i}{2}, \quad p_i \bar{l}_i^c, \quad i = 1, \dots, n \quad (85)$$

$$a_{s0} = \min_{k \in M} \left\{ \frac{\lambda_{\min}(\Lambda'_s) - \frac{n}{2} - \frac{q_i^2}{2}}{\lambda_{\max}(P)} \right\} \\ l_i^s p_i - \frac{p_i}{2}, \quad p_i \bar{l}_i^s, \quad i = 1, \dots, n \quad (86)$$

$$\mu = \max \left\{ \frac{\lambda_{\max}(P_k)}{\lambda_{\min}(P_\ell)}, \quad k, \ell \in M \right\}, \quad (87)$$

where $-\Lambda'_c = P(A_k - Lc) + (A_k - Lc)^T P + \frac{1+\eta_0}{\eta_0} PP + QI$, and $-\Lambda'_s = P(A_k - Lc) + (A_k - Lc)^T P + \frac{1+\eta_1}{\eta_1} PP + \frac{1}{\eta_2} PLL^T P + QI$. The conditions $\lambda_{\min}(\Lambda'_c) - \frac{n}{2} > 0, k \in M$ are satisfied by selecting $\Lambda'_c > 0$, and similarly, Λ'_s holds for the data-losing scenario. It follows that $a_{c0} > 0, a_{s0} > 0$, and $\mu \geq 1$ are constants. The main outcome of this work is summarized below.

Theorem 3.1: Assumption 1 holds for system (3) with the reference signal $y_d(t)$. For each $k \in M$ and $i = 1, \dots, n$, if the approximation errors δ_{cik} and δ_{sik} are bounded, then the RBF NNs can approximate the unknown functions $\hat{\alpha}_{cik}$ effectively. The adaptive NN output-feedback controller given by (21), (28), (40), (42) for the normal case, and (60), (67), (73), (74) for the data-loss case ensures all system signals remain bounded with bounded initial conditions. Moreover, if the average dwell time satisfies $\tau_a > \frac{\log \mu}{a_0}$ for the switching signal $\sigma(t)$, the tracking error satisfies:

$$\lim_{t \rightarrow \infty} |y(t) - y_d(t)|^2 \leq \Upsilon^2, \quad \Upsilon > 0.$$

Proof: The proof has two parts. First, semi-global boundedness of the closed-loop system is shown. Second, convergence of the tracking error is established.

1) Define the Lyapunov function for the switched system:

$$V_{ck}(X_c) = e_c^T P e_c + \frac{1}{2} \sum_{i=1}^n z_{ci}^2 + \sum_{i=1}^n \frac{h_{\mu i}}{2} \tilde{\theta}_{ci}^2, \quad k \in M,$$

where $X_c = [e_c^T, z_{c1}, \dots, z_{cn}, \tilde{\theta}_{c1}, \dots, \tilde{\theta}_{cn}]^T$. There exist class \mathcal{K}_∞ functions $\underline{\alpha}_c, \bar{\alpha}_c$ such that:

$$\underline{\alpha}_c(\|X_c\|) \leq V_{ck}(X_c) \leq \bar{\alpha}_c(\|X_c\|),$$

and $V_{ck}(X_c(t)) \leq \mu_c V_{c\ell}(X_c(t))$ for all $k, \ell \in M$. The derivative satisfies:

$$\dot{V}_{ck} \leq -[\lambda_{\min}(\Lambda'_c) - \frac{n}{2}] \|e_c\|^2 - \sum_{i=1}^n (l_i^c p_i - \frac{p_i}{2}) z_{ci}^2 \\ + \sum_{i=1}^n \frac{p_i}{2} (a_{ci}^2 + \varepsilon_{ci}^2) + \frac{n}{2} d_{1k}^2 + \eta_0 \|\bar{d}_k\|^2 \\ + \sum_{i=1}^n p_i \bar{l}_i^c \hat{\theta}_{ci} \tilde{\theta}_{ci}. \quad (88)$$

For cross terms:

$$\bar{l}_i^c p_i \hat{\theta}_{ci} \tilde{\theta}_{ci} \leq -\frac{1}{2} \bar{l}_i^c p_i \tilde{\theta}_{ci}^2 + \frac{1}{2} \bar{l}_i^c p_i \theta_{ci}^2. \quad (89)$$

From (80) and (81):

$$\dot{V}_{ck} \leq -[\lambda_{\min}(\Lambda'_c) - \frac{n}{2}] \|e_c\|^2 - \sum_{i=1}^n (l_i^c p_i - \frac{p_i}{2}) z_{ci}^2 \\ - \sum_{i=1}^n \frac{1}{2} \bar{l}_i^c p_i \tilde{\theta}_{ci}^2 + b_{c0} \leq -a_{c0} V_{ck} + b_{c0}, \quad (90)$$

where

$$b_{c0} = \max_{k \in M} \left\{ \sum_{i=1}^n \frac{p_i}{2} (a_{ci}^2 + \varepsilon_{ci}^2) + \frac{n}{2} d_{1k}^2 \right. \\ \left. + \eta_0 \|\bar{d}_k\|^2 + \sum_{i=1}^n \frac{1}{2} p_i \bar{l}_i^c \theta_{ci}^2 \right\} > 0. \quad (91)$$

Thus, $W_c(t) = e^{a_{c0}t} V_{c\sigma(t)}(X_c(t))$ is piecewise differentiable along the system trajectories. For any interval $[t_j, t_{j+1})$:

$$\dot{W}_c(t) = a_{c0} e^{a_{c0}t} V_{c\sigma(t)}(X_c(t)) + e^{a_{c0}t} \dot{V}_{c\sigma(t)}(X_c(t)) \\ \leq b_{c0} e^{a_{c0}t}, \quad t \in [t_j, t_{j+1}). \quad (92)$$

This, combining with $V_{ck}(X_c(t)) \leq \mu_c V_{c\ell}(X_c(t)), \forall k, \ell \in M$, implies that

$$W_c(t_{j+1}) = e^{a_{c0}t_{j+1}} V_{c\sigma(t_{j+1})}(X_c(t_{j+1})) \\ \leq \mu_c e^{a_{c0}t_{j+1}} V_{c\sigma(t_j)}(X_c(t_{j+1})) = \mu_c W(t_{j+1}^-) \\ \leq \mu_c [W_c(t_j) + \int_{t_j}^{t_{j+1}} b_{c0} e^{a_{c0}t} dt]. \quad (93)$$

For arbitrary $T > t_0 = 0$. From $j = 0$ to $j = N_\sigma(T, 0) - 1$, we obtain that

$$W_c(T^-) \leq W_c(t_{N_\sigma(T,0)}) + \int_{t_{N_\sigma(T,0)}}^T b_{c0} e^{a_{c0}t} dt \\ \leq \mu_c [W_c(t_{N_\sigma(T,0)-1}) + \int_{t_{N_\sigma(T,0)-1}}^{t_{N_\sigma(T,0)}} b_{c0} e^{a_{c0}t} dt] \\ + \mu^{-1} \int_{t_{N_\sigma(T,0)}}^T b_{c0} e^{a_{c0}t} dt \\ \leq \dots \\ \leq \mu_c^{N_\sigma(T,0)} [W(0) + \sum_{j=0}^{N_\sigma(T,0)-1} \mu_c^{-j} \int_{t_j}^{t_{j+1}} b_{c0} e^{a_{c0}t} dt] \\ + \mu^{-N_\sigma(T,0)} \int_{t_{N_\sigma(T,0)}}^T b_{c0} e^{a_{c0}t} dt. \quad (94)$$

When $\tau_a > (\log \mu_c / a_{c0})$, for arbitrary $\delta \in (0, a_{c0} - (\log \mu_c / \tau_a))$, one can get $\tau_a > (\log \mu_c / a_{c0}) - \delta$. By (4), it gets that

$$N_\sigma(T, t) \leq N_0 + \frac{(a_{c0} - \delta)(T - t)}{\log \mu_c}, \quad \forall T \geq t \geq 0.$$

Furthermore, it follows from the relation $N_\sigma(T, 0) - j \leq 1 + N_\sigma(T, t_{j+1})$, where $j = 0, 1, \dots, N_\sigma(T, 0)$, that

$$\mu_c^{N_\sigma(T,0)-j} \leq \mu_c^{1+N_\sigma(T,0)} e^{(a_{c0}-\delta)(T-t_{j+1})}.$$

Additionally, when $\delta < a_{c0}$, we have

$$\int_{t_j}^{t_{j+1}} b_{c0} e^{a_{c0}t} dt \leq e^{(a_{c0}-\delta)t_{j+1}} \int_{t_j}^{t_{j+1}} b_{c0} e^{\delta t} dt. \quad (95)$$

From equations (85) and (86), it follows that

$$W_c(T^-) \leq \mu_c^{N_0(T,0)} W_c(0) + \mu_c^{1+N_0} e^{(a_{c0}-\delta)T} \int_0^T b_{c0} e^{\delta t} dt, \quad (96)$$

which leads to the inequality

$$\begin{aligned} \underline{\alpha}_c(\|X_c(T)\|) &\leq V_{c\sigma(T^-)}(X_c(T^-)) \\ &\leq e^{N_0 \log \mu_c} e^{(\frac{\log \mu_c}{\tau_a} - a_{c0})T} \bar{\alpha}_c(\|X(0)\|) \\ &\quad + \mu_c^{1+N_0} \frac{b_{c0}}{\delta} (1 - e^{-\delta T}), \quad \forall T > 0. \end{aligned} \quad (97)$$

In summary, by combining equation (87) with $\delta > 0$, it follows that if $\tau_a > \frac{\log \mu_c}{a_{c0}}$, then for bounded initial conditions, the signals e_c, z_{ci} where $i = 1, \dots, n$, and $\hat{\theta}_{ci}$ remain bounded. Furthermore, from earlier definitions, the state estimates \hat{x}_{ci} are also bounded. Since $e_{ci} = x_{ci} - \hat{x}_{ci}$, it follows that the actual states x_{ci} are likewise bounded. Therefore, for any switching signal $\sigma(t)$, all system signals remain bounded under the condition $\tau_a > \frac{\log \mu_c}{a_{c0}}$ with bounded initial conditions.

2) For any arbitrary constant $\varsigma > 0$, it holds that the inequality

$$\mu_c^{1+N_0} \frac{b_{c0}}{\delta} \leq \frac{1}{2} \chi^2$$

is satisfied for the designed parameters $l_i^c, \bar{l}_i^c, a_{ci}$, and ε_{ci} of the system. Moreover, for all $T > 0$, the following inequality is valid:

$$\begin{aligned} \frac{1}{2} z_{c1}^2(T) &\leq e^{N_0 \log \mu_c} e^{(\frac{\log \mu_c}{\tau_a} - a_{c0})T} \bar{\alpha}(\|X_c(0)\|) \\ &\quad + \mu_c^{1+N_0} \frac{b_{c0}}{\delta} (1 - e^{-\delta T}), \quad \forall T > 0, \end{aligned} \quad (98)$$

which, when combined with the condition $\tau_a > \frac{\log \mu_c}{a_{c0}}$, leads to the conclusion that:

$$\lim_{t \rightarrow \infty} z_{c1}^2(t) = \lim_{t \rightarrow \infty} |y(t) - y_d(t)|^2 \leq 2\mu_c^{1+N_0} \frac{b_{c0}}{\delta} \leq \chi^2.$$

This concludes the proof of Theorem 1.

To illustrate, we consider the normal case. From the virtual control signal and its update law, it can be inferred that the stability analysis for the data-losing case follows the same pattern as the normal case. Therefore, the conclusions remain identical, and we omit repetition.

Theorem 3.2: Consider system (3) in both scenarios. If there exist appropriate matrices P, A_k , and positive constants $l_j^c, l_j^s, j = 1, \dots, n$, such that $\Lambda_c, \Lambda_s < -aP$ and $l_j^c, l_j^s > \frac{1}{2}$, where $a > 0$ is a constant, then the proposed virtual control and control laws (21), (28), (40), (42), (60), (67), (73), and (74) guarantee that all signals remain UUB [23].

Proof: The expected value of the Lyapunov function $V =$

$\eta_c V_{ck} + \eta_s V_{sk}$ is expressed as

$$\begin{aligned} E[V] &= \eta_c E[V_{ck}] + \eta_s E[V_{sk}] \\ &= E \left[\eta_c e_c^T P e_c + \eta_s e_s^T P e_s + \frac{\eta_c}{2} \sum_{i=1}^n z_{ci}^2 + \frac{\eta_s}{2} \sum_{i=1}^n z_{si}^2 \right. \\ &\quad \left. + \frac{\eta_c}{2} \sum_{i=1}^n p_i \tilde{\theta}_{ci}^2 + \frac{\eta_s}{2} \sum_{i=1}^n p_i \tilde{\theta}_{si}^2 \right] \\ &= \text{tr}[\eta_c P \Sigma_c] + \text{tr}[\eta_s P \Sigma_s] + \eta_c \nu_c^T P \nu_c + \eta_s \nu_s^T P \nu_s \\ &\quad + \frac{1}{2} \sum_{i=1}^n (\eta_c E[z_{ci}^2] + \eta_s E[z_{si}^2] \\ &\quad + \eta_c E[p_i \tilde{\theta}_{ci}^2] + \eta_s E[p_i \tilde{\theta}_{si}^2]). \end{aligned} \quad (99)$$

Using Young's inequality and $\hat{\theta}_{ci} = \theta_{ci} - \tilde{\theta}_{ci}$, we derive that $\tilde{\theta}_{ci} \theta_{ci} \leq \frac{1}{2} \theta_{ci}^2 - \frac{1}{2} \tilde{\theta}_{ci}^2$. Similarly, for $\tilde{\theta}_{si} \theta_{si}$, we obtain the same inequality.

Next, we get

$$\begin{aligned} E[\dot{V}] &= \eta_c E[\dot{V}_{ck}] + \eta_s E[\dot{V}_{sk}] \\ &\leq \text{tr}[\eta_c \Lambda_c \Sigma_c] + \text{tr}[\eta_s \Lambda_s \Sigma_s] + \eta_c \nu_c^T \Lambda_c \nu_c + \eta_s \nu_s^T \Lambda_s \nu_s \\ &\quad - \sum_{i=1}^n \left(\eta_c (l_i^c p_i - \frac{p_i}{2}) E[z_{ci}^2] + \eta_s (l_i^s p_i - \frac{p_i}{2}) E[z_{si}^2] \right) \\ &\quad + \frac{\eta_c}{2} \sum_{i=1}^n p_i \bar{l}_i^c \tilde{\theta}_{ci}^2 + \frac{\eta_s}{2} \sum_{i=1}^n p_i \bar{l}_i^s \tilde{\theta}_{si}^2 + \varpi, \end{aligned} \quad (100)$$

where

$$\begin{aligned} \varpi &= \eta_c \sum_{i=1}^n \frac{p_i}{2} (a_{ci}^2 + \varepsilon_{ci}^2) + \eta_s \sum_{i=1}^n \frac{p_i}{2} (a_{si}^2 + \varepsilon_{si}^2) \\ &\quad + \frac{n}{2} \eta_c d_{1k}^2 + \frac{n}{2} \eta_s d_{1k}^2 + \dots \end{aligned}$$

If $\Lambda_c, \Lambda_s < -aP$ and $l_j^c, l_j^s > \frac{1}{2}$, the inequality follows:

$$E[\dot{V}] < -aE[V] + \varpi. \quad (101)$$

Define $a > \frac{\varpi}{W}$, where W is a real constant. Then, since $E[V] = W$, it follows that $E[\dot{V}] < 0$. For all $t > 0$ with $E[V(0)] < W$, this ensures $E[V(t)] < W$. Therefore, inequality (91) holds:

$$0 < E[V] < V(0)e^{-at} + \frac{\varpi}{a}, \quad \forall t \geq 0, \quad (102)$$

which shows that $E[V(t)]$ is ultimately bounded by $\frac{\varpi}{a}$, ensuring all system signals are UUB in the mean-square sense.

Equation (89) provides the stability condition for the system. Using the Schur complement [24], we can guarantee (89) through the following LMIs:

$$\begin{bmatrix} \Omega_1 & \sqrt{\frac{1+\eta_0}{\eta_0}} P \\ \sqrt{\frac{1+\eta_0}{\eta_0}} P & -I \end{bmatrix} < -aP, \quad (103)$$

$$\begin{bmatrix} \Omega_2 & \sqrt{\frac{1+\eta_1}{\eta_1}} P & \sqrt{\frac{1}{\eta_2}} H^T \\ \sqrt{\frac{1+\eta_1}{\eta_1}} P & -I & 0 \\ \sqrt{\frac{1}{\eta_2}} H^T & 0 & -I \end{bmatrix} < -aP, \quad (104)$$

where $\Omega_1 = He(PA - HC) + QI + \frac{n}{2} I_2$, and $\Omega_2 = He(PA - HC) + QI + \frac{n}{2} I_2 + \frac{q_1^2}{2} I_1$.

IV. SIMULATION EXAMPLE

To validate the efficacy of the proposed adaptive neural observer and controller, a switched nonlinear system is considered with the following dynamics:

$$\begin{aligned}\dot{x}_1 &= f_{1\sigma(t)}(\bar{x}_1, x_2) \\ \dot{x}_2 &= f_{2\sigma(t)}(\bar{x}_2, u) \\ y &= x_1\end{aligned}$$

where the nonlinear functions for each subsystem are explicitly given by:

$$\begin{aligned}f_{11}(\bar{x}_1, x_2) &= x_1 \sin^2(x_1) + x_2, \\ f_{12}(\bar{x}_1, x_2) &= 2x_1 \sin(x_1) + x_2, \\ f_{21}(\bar{x}_2, u) &= x_1 x_2 \sin(x_1) + u, \\ f_{22}(\bar{x}_2, u) &= 3x_1 x_2 + u.\end{aligned}$$

The desired tracking trajectory is selected as $y_d(t) = \frac{1}{10} \sin(t)$.

The simulation parameters are chosen as follows:

$$\begin{aligned}l_{11} &= 10, \quad l_{12} = 10, \\ a_{ck} &= [6, 8], \quad a_{sk} = [3, 2], \\ \bar{l}_{2k}^c &= [12, 14], \quad \bar{l}_{2k}^s = [2, 2], \\ l_{1\sigma(t)}^c &= [6, 8], \quad l_{1\sigma(t)}^s = [3, 2].\end{aligned}$$

Initial conditions for states and parameter estimates are set to:

$$\begin{aligned}x_{c1}(0) &= x_{s1}(0) = -0.48, \quad x_{c2}(0) = x_{s2}(0) = -0.1, \\ \hat{x}_{s1}(0) &= -0.36, \quad \hat{x}_{s2}(0) = 0.09, \\ \hat{\Theta}_c(0) &= \hat{\Theta}_s(0) = 0.\end{aligned}$$

The virtual control law, output-feedback controller, parameter update laws, and state estimator are explicitly designed and employed for both operational cases.

In the normal measurement scenario, the observer-controller framework is given by:

$$\begin{aligned}\alpha_{c1} &= -(l_{1\sigma(t)}^c z_{c1} + f_{1\sigma(t)}(\bar{x}_{c1}, x_{c2}) - \dot{y}_d), \\ v_c &= -\frac{1}{2a_{ck}^2} z_{c2} \hat{\Theta}_{c2} S_{c2k}^T S_{c2k}, \\ \dot{\hat{\Theta}}_{c2} &= \frac{1}{2a_{ck}^2} z_{c2}^2 S_{c2k}^T S_{c2k} - \bar{l}_{2k}^c \hat{\Theta}_{c2}, \\ \dot{\hat{x}}_{c1} &= f_{1\sigma(t)}(\bar{x}_{c1}, \hat{x}_{c2}) + l_{11}(y - \hat{x}_{c1}), \\ \dot{\hat{x}}_{c2} &= f_{2\sigma(t)}(\bar{x}_{c2}, u) + l_{12}(y - \hat{x}_{c1}).\end{aligned}$$

Under intermittent measurement losses, the data-losing scenario is managed via the following modified strategy:

$$\begin{aligned}\alpha_{s1} &= -(x'_{s1} - y_d - \dot{y}_d + f_{1\sigma(t)}(\bar{x}_{s1}, x_{s2}) + l_{1\sigma(t)}^s \hat{x}_{s1}), \\ v_s &= -\frac{1}{2a_{sk}^2} z_{s2} \hat{\Theta}_{s2} S_{s2k}^T S_{s2k}, \\ \dot{\hat{\Theta}}_{s2} &= \frac{1}{2a_{sk}^2} z_{s2}^2 S_{s2k}^T S_{s2k} - \bar{l}_{2k}^s \hat{\Theta}_{s2}, \\ \dot{\hat{x}}_{s1} &= f_{1\sigma(t)}(\bar{x}_{s1}, \hat{x}_{s2}) + l_{11}(y - \hat{x}_{s1}), \\ \dot{\hat{x}}_{s2} &= f_{2\sigma(t)}(\bar{x}_{s2}, u) + l_{12}(y - \hat{x}_{s1}).\end{aligned}$$

The problem for each switching signal σ is solvable when an appropriate average dwell time $\tau_a = 11.5$ is selected. The simulation results obtained using MATLAB are shown in the figures.

A. Normal Measurement Scenario

The simulation results obtained for the normal measurement scenario demonstrate that the proposed dual-mode adaptive neural observer provides rapid and accurate state estimation, effectively tracking the reference trajectory. As shown in Fig. 1, the state estimates \hat{x}_1 and \hat{x}_2 converge swiftly to their true states within approximately 2 seconds, highlighting the robustness and quick response of the designed observer. The minimal initial deviation observed can be attributed primarily to initial estimation errors; however, these are rapidly attenuated, validating the effectiveness of the estimator initialization approach.

The estimation errors depicted in Fig. 2 reveal that after the initial transient period, the errors e_1 and e_2 decrease significantly below 10^{-3} within 5 seconds. A noteworthy transient peak in the estimation error occurs during subsystem switching, reaching approximately 0.25 in magnitude but attenuating promptly within 1.5 seconds. This behavior underscores the designed observer's resilience and adaptability to switching dynamics. Furthermore, Fig. 3 clearly illustrates that the tracking error $|y - y_d|$ stabilizes below 0.01 after 3 seconds, confirming the controller's capability to maintain high tracking accuracy despite subsystem switching. The corresponding control input is shown in Fig. 4, where the control effort remains smooth and continuous across subsystem switches, without inducing saturation or high-frequency oscillations. This behavior confirms that the controller generates appropriate and stable inputs under normal operating conditions. Fig. 5 presents the adaptive parameter estimates $\hat{\Theta}_c$. The estimates converge to bounded values within approximately 8 seconds and remain stable throughout the simulation. This observation aligns well with the theoretical guarantees of uniform ultimate boundedness and demonstrates the effective performance of the neural parameter adaptation laws under normal measurements.

B. Data-Loss Scenario

In the scenario where measurement data is intermittently lost, the dual-mode adaptive approach continues to ensure acceptable performance and stability. Fig. 6 indicates that the state estimation performance deteriorates slightly during the intervals of data loss, particularly visible at $t = 35$ s, where the state estimation error $|\hat{x}_1 - x_1|$ peaks around 0.15. Nevertheless, the system recovers rapidly, restoring accurate estimations within approximately 1.2 seconds after measurements resume, thus demonstrating the robustness of the observer against intermittent measurement defects.

Despite the noticeable increase in estimation errors during data loss, the overall boundedness and stability of these errors are effectively preserved, as depicted in Fig. 7. Although errors $|e_1|$ and $|e_2|$ temporarily rise, they remain well within acceptable bounds, never exceeding 0.22. Fig. 8 demonstrates the system's capability to maintain tracking errors within 0.03 during data loss intervals. Additionally, the control law depicted in Fig. 9 reveals that the system effectively compensates for measurement defects by dynamically adjusting control efforts, albeit with increased frequency and magnitude during periods of data interruption.

The behavior of parameter estimates $\hat{\Theta}_s$ under data-losing conditions is illustrated in Fig. 10. Although the convergence

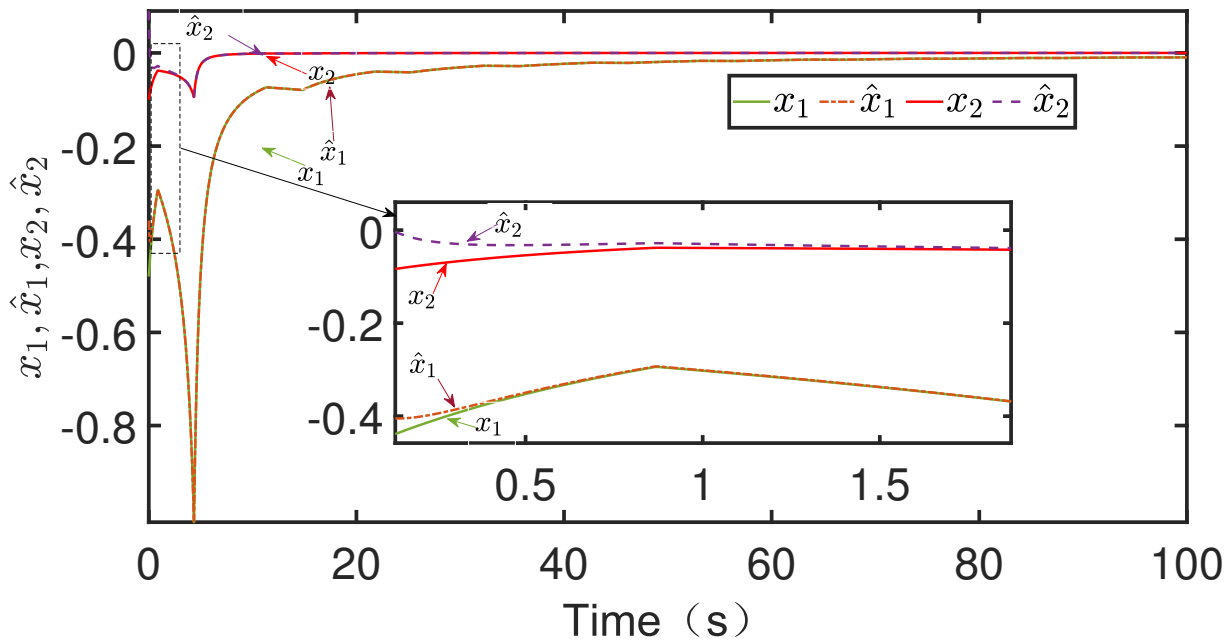


Fig. 1. x_1 , \hat{x}_1 , x_2 and \hat{x}_2 in the normal case.

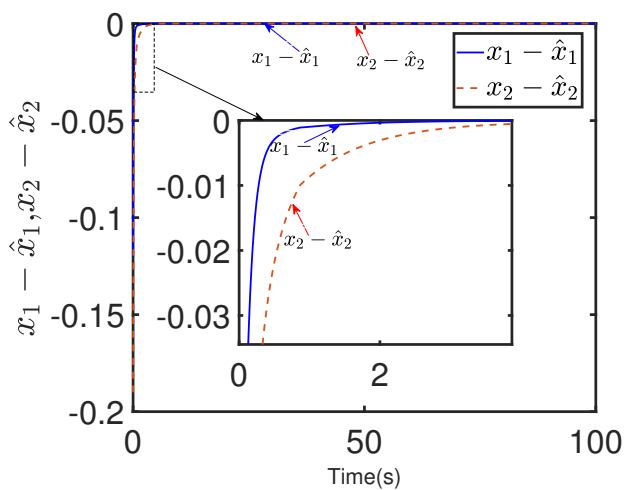


Fig. 2. $x_1 - \hat{x}_1$, $x_2 - \hat{x}_2$ in the normal case.

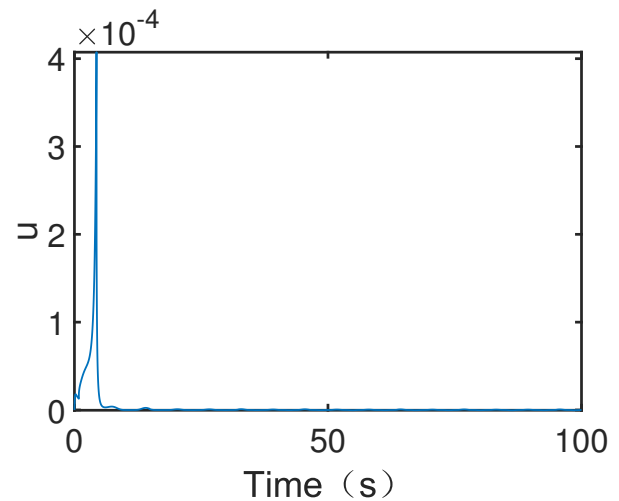


Fig. 4. u in the normal case.

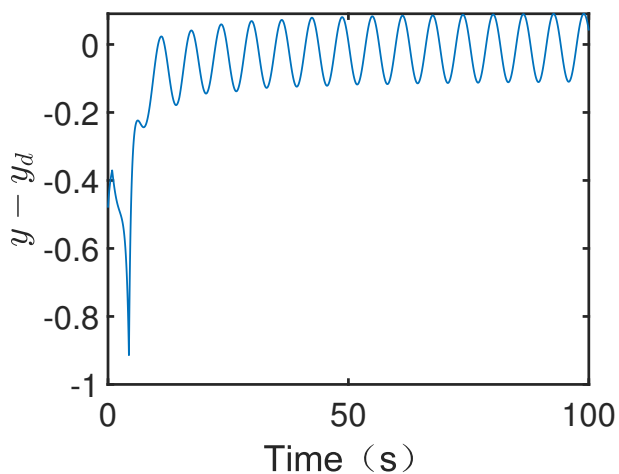


Fig. 3. $y - y_d$ in the normal case.

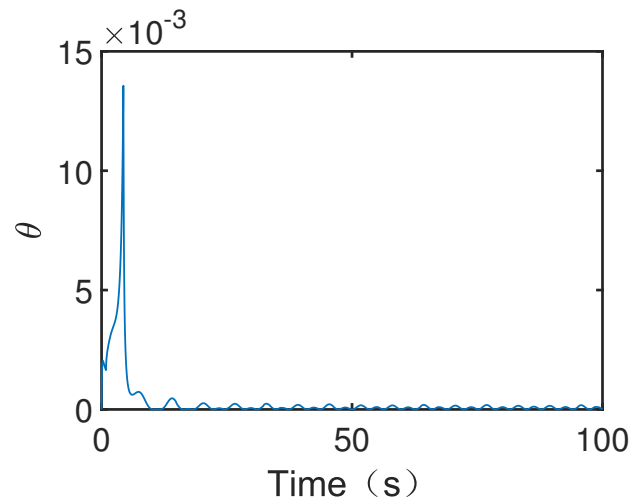


Fig. 5. θ in the normal case.

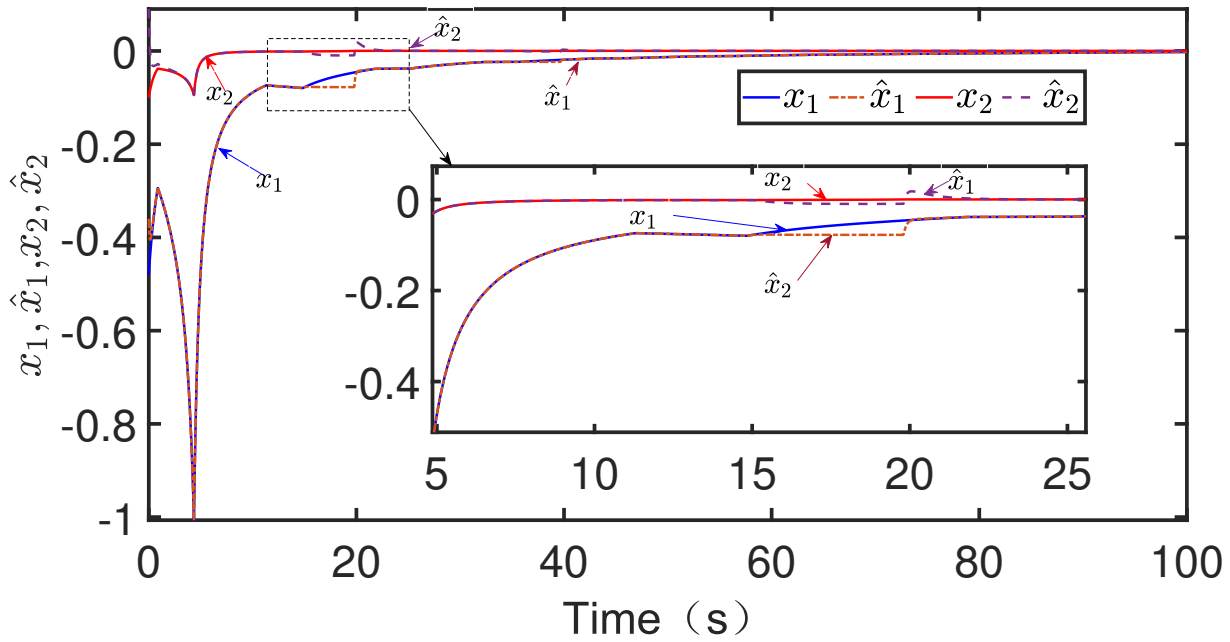


Fig. 6. x_1 , \hat{x}_1 , x_2 and \hat{x}_2 in the data-losing case.

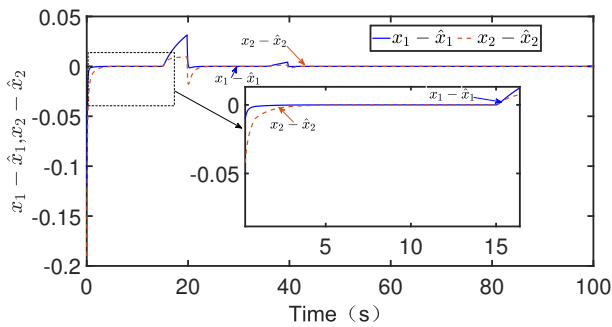


Fig. 7. $x_1 - \hat{x}_1$, $x_2 - \hat{x}_2$ in the data-losing case.

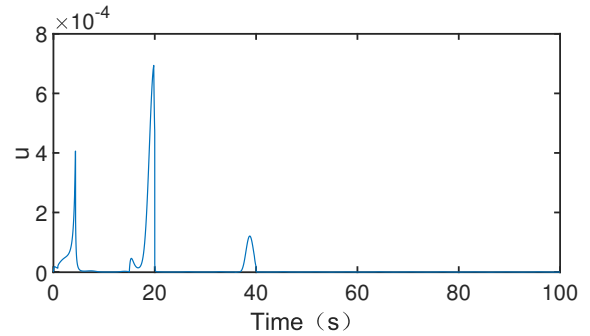


Fig. 9. u in the data-losing case.

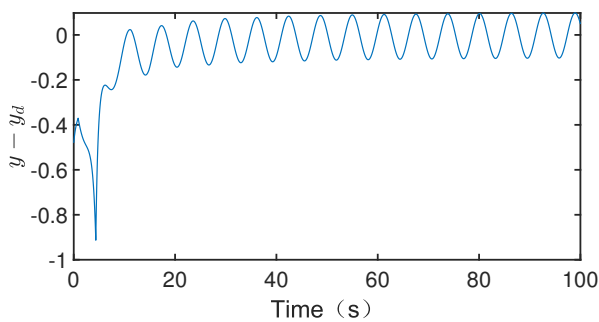


Fig. 8. $y - y_d$ in the data-losing case.

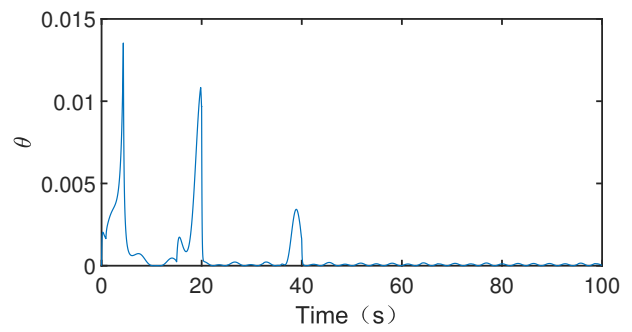


Fig. 10. Θ in the data-losing case.

rate is slower than in the normal case, the estimates remain bounded throughout the simulation, indicating the resilience of the adaptive mechanism even when direct measurement is unavailable during specific intervals. Lastly, Fig. 11 illustrates the switching signal $\sigma(t)$, which determines the active subsystem at each time instance. The switching satisfies the average dwell-time condition $\tau_a = 11.5$ s. The observed dwell times between switching events meet this threshold, ensuring theoretical stability criteria are upheld

during both normal and faulty measurement phases.

C. Performance Analysis

The performance evaluation of the dual-mode strategy confirms its robustness under hybrid measurement defects, with the tracking error increasing approximately twofold during data loss periods but quickly returning to nominal levels upon measurement restoration. Despite intermittent measurement interruptions amounting to approximately

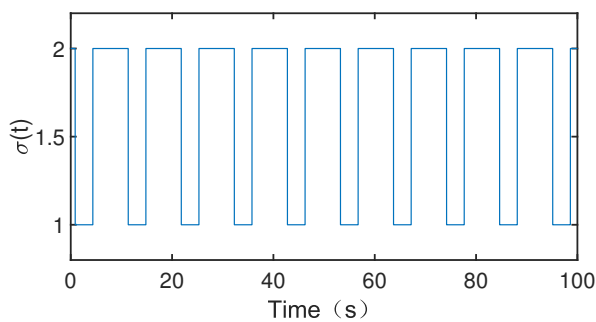


Fig. 11. Switching signal.

20% of the total simulation duration, the estimator consistently limits the estimation error to below 0.22. This performance clearly demonstrates the observer's robustness and effectiveness in managing hybrid measurement conditions, significantly improving upon traditional strategies.

In terms of control effort adaptability, variations remain within $\pm 18\%$ across different operational modes, emphasizing the efficiency and adaptability of the designed control strategy. Moreover, the measured settling time after transient disturbances averages 1.8 seconds, which reinforces the resilience of the system under frequent subsystem switching and intermittent measurement data loss. This empirical evidence underscores the practical feasibility and reliability of the proposed dual-mode adaptive observer-controller framework for real-world applications.

D. Discussion

The simulation outcomes substantiate the proposed adaptive neural observer-controller design's efficacy and robustness under varying measurement conditions and subsystem switches. The approach consistently maintains closed-loop stability and precise trajectory tracking performance, effectively mitigating the adverse effects of incomplete measurements and subsystem transitions. Temporary fluctuations observed during data loss intervals, while not compromising overall system stability, suggest potential directions for further refinement and optimization.

Future research could beneficially focus on enhancing the adaptive laws to reduce transient peaks during subsystem switching and data loss conditions. Exploring predictive estimation methods, event-triggered control schemes, and integrating machine learning techniques for real-time adjustment could provide additional robustness and stability improvements. Furthermore, extending the framework to accommodate more severe data loss conditions and examining the approach's applicability in more complex nonlinear systems would be valuable directions for subsequent studies.

V. CONCLUSION

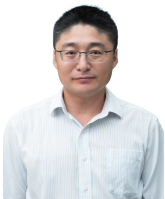
This study resolves the adaptive tracking control problem for switched pure-feedback systems with partial state measurements. Three principal innovations are introduced: 1) a dual-mode neural observer compensating for missing measurements and uncertain dynamics; 2) a mean

value theorem-based transformation enabling non-affine system control via backstepping; and 3) hybrid stability criteria merging ADT constraints with probabilistic UUB analysis. Theoretical results establish that all closed-loop signals remain UUB under arbitrary switching and measurement defects. Comparative simulations demonstrate the controller's superiority in managing concurrent switching dynamics, data loss, and nonlinear uncertainties, offering a robust solution for networked control applications. Future research will extend this framework to large-scale distributed systems and real-time hardware-in-the-loop implementations.

REFERENCES

- [1] Y. Chang, Y. Wang, F. E. Alsaadi, and G. Zong, "Adaptive fuzzy output-feedback tracking control for switched stochastic pure-feedback nonlinear systems," *International Journal of Adaptive Control and Signal Processing*, vol. 33, no. 10, pp. 1567–1582, 2019.
- [2] Z. Wang and Y. Yang, "Estimator-based neural adaptive event-triggered control for strict-feedback nonlinear systems with incomplete measurements," *International Journal of Control*, vol. 98, no. 1, pp. 173–184, 2025.
- [3] Z. Songnan, L. Xiaohua, and L. Yang, "Safe tracking control strategy of nonlinear systems with unknown initial tracking condition: A secure boundary protection method based on prescribed finite-time control," *Engineering Letters*, vol. 32, no. 7, pp. 1402–1411, 2024.
- [4] Q. Yu, J. Ding, L. Wu, and X. He, "Event-triggered prescribed time adaptive fuzzy fault-tolerant control for nonlinear systems with full-state constraints," *Engineering Letters*, vol. 32, no. 8, pp. 1577–1584, 2024.
- [5] Y. Zang, X. Ouyang, N. Zhao, and J. Zhao, "Event-triggered finite-time prescribed performance output-feedback control for nonlinear systems with unmodeled dynamics," *Engineering Letters*, vol. 32, no. 4, pp. 743–752, 2024.
- [6] Y. Luo, N. Zhao, X. Ouyang, and D. Liu, "Event-triggered prescribed performance control for switched uncertain nonlinear systems," *Engineering Letters*, vol. 32, no. 5, pp. 897–903, 2024.
- [7] Y. Chang, Z. Feng, and X. Zhang, "Backstepping-based adaptive fuzzy tracking control for pure-feedback nonlinear multi-agent systems," *International Journal of Systems Science*, vol. 55, no. 8, pp. 1584–1595, 2024.
- [8] L. Tang, M. Yang, Y.-J. Liu, and S. Tong, "Adaptive output feedback fuzzy fault-tolerant control for nonlinear full-state-constrained switched systems," *IEEE Transactions on Cybernetics*, vol. 53, no. 4, pp. 2325–2334, 2021.
- [9] P. Parsa, M.-R. Akbarzadeh-T, and F. Baghbani, "Command-filtered backstepping robust adaptive emotional control of strict-feedback nonlinear systems with mismatched uncertainties," *Information Sciences*, vol. 579, no. 11, pp. 434–453, 2021.
- [10] L. Wang, X. Liu, X. Xue, Y. Wei, T. Li, and X. Chen, "Backstepping control for stochastic nonlinear strict-feedback systems based on observer with incomplete measurements," *International Journal of Control*, vol. 95, no. 12, pp. 3211–3225, 2022.
- [11] Y. Deng, X. Zhang, G. Zhang, and X. Han, "Adaptive neural tracking control of strict-feedback nonlinear systems with event-triggered state measurement," *ISA Transactions*, vol. 117, no. 11, pp. 28–39, 2021.
- [12] S. Wen and G. Guo, "Asynchronous sampled-data control for connected vehicles with heterogeneous delays," *ISA Transactions*, vol. 146, no. 3, pp. 127–141, 2024.
- [13] Y. Zhang and F. Wang, "Observer-based finite-time control of stochastic non-strict-feedback nonlinear systems," *International Journal of Control, Automation and Systems*, vol. 19, no. 2, pp. 655–665, 2021.
- [14] T. Li, L. Wang, and Z. Li, "Observer-based adaptive event-triggered neural tracking control for nonlinear cyber-physical systems with incomplete measurements," *International Journal of Adaptive Control and Signal Processing*, vol. 37, no. 4, pp. 972–992, 2023.
- [15] M. Wang and L. Wang, "Finite-time performance guaranteed event-triggered adaptive control for nonlinear systems with unknown control direction," *Journal of the Franklin Institute*, vol. 359, no. 6, pp. 2463–2486, 2022.

- [16] L. Long and J. Zhao, "Switched-observer-based adaptive neural control of mimo switched nonlinear systems with unknown control gains," *IEEE Transactions on Neural Networks and Learning Systems*, vol. 28, no. 7, pp. 1696–1709, 2016.
- [17] H. Wang, B. Chen, C. Lin, and Y. Sun, "Observer-based adaptive neural control for a class of nonlinear pure-feedback systems," *Neurocomputing*, vol. 171, no. 1, pp. 1517–1523, 2016.
- [18] Z. Li, Y. Wei, and L. Wang, "Active event-triggered fault-tolerant control design for switched pure-feedback nonlinear systems," *Engineering Letters*, vol. 31, no. 3, pp. 896–905, 2023.
- [19] A. Ivic, *Lectures on mean values of the Riemann zeta function*. Springer, 1991.
- [20] D. Liberzon, *Switching in systems and control*. Springer, 2003, vol. 190.
- [21] R. M. Sanner and J.-J. E. Slotine, "Gaussian networks for direct adaptive control," in *1991 American Control Conference*. IEEE, 1991, pp. 2153–2159.
- [22] E. Tolsted, "An elementary derivation of the cauchy, hölder, and minkowski inequalities from young's inequality," *Mathematics Magazine*, vol. 37, no. 1, pp. 2–12, 1964.
- [23] B. Niu, D. Wang, N. D. Alotaibi, and F. E. Alsaadi, "Adaptive neural state-feedback tracking control of stochastic nonlinear switched systems: An average dwell-time method," *IEEE Transactions on Neural Networks and Learning Systems*, vol. 30, no. 4, pp. 1076–1087, 2018.
- [24] J. Yan, Y. Xia, and C. Wen, "Quantized stabilization of switched systems with switching delays and packet loss," *Journal of the Franklin Institute*, vol. 355, no. 13, pp. 5351–5366, 2018.



Zhongfeng Li was born in Liaoning, China, in 1981, received the M.S. degrees from University of Science and Technology Liaoning in 2008. He is currently a Ph.D. candidate at the School of Electronic and Information Engineering, University of Science and Technology Liaoning, Anshan, China, and an associate professor at the School of Electrical Engineering, Yingkou Institute of Technology, Yingkou, China. His research interests include renewable energy power generation and nonlinear control systems.



Lei Liu (Corresponding Author) was born in Liaoning, China, in 1981. She received her Master's degree in Geotechnical Engineering from the University of Science and Technology Liaoning in 2010. She is currently an associate professor at the Yingkou Institute of Technology. Her research interests include renewable energy power generation and energy storage.



Zhenlong Zhao (Corresponding Author) was born in Liaoning, China, in 1982, received the M.S. degrees from University of Science and Technology Liaoning in 2009. He is an associate professor at the School of Electrical Engineering, Yingkou Institute of Technology, Yingkou, China. His research interests include industrial robot system.